J. Fluid Mech. (1996), vol. 327, pp. 273–301

Diffusional–thermal instability of diffusion flames

By J. S. KIM[1],† F. A. WILLIAMS[1] AND P. D. RONNEY[2]

[1]Center for Energy and Combustion Research, Department of Applied Mechanics and Engineering Sciences, University of California, San Diego, La Jolla, CA 92093-0411, USA

[2]Department of Mechanical Engineering, University of Southern California, Los Angeles, CA 90089-1453, USA

(Received 17 May 1995 and in revised form 9 May 1996)

The diffusional–thermal instability, which gives rise to striped quenching patterns that have been observed for diffusion flames, is analysed by studying the model of a one-dimensional convective diffusion flame in the diffusion-flame regime of activation-energy asymptotics. Attention is focused principally on near-extinction conditions with Lewis numbers less than unity, in which the reactants with high diffusivity diffuse into the strong segments of the reaction sheet, so that the regions between the strong segments become deficient in reactant and subject to the local quenching that leads to the striped patterns. This analysis differs from other flame stability analyses in that the complete description of the dispersion relation is obtained from a composite expansion of the results of an analysis with the conventional convective–diffusive scaling and one with reaction-zone scaling. The results predict that striped patterns will occur, for flames sufficiently close to quasi-steady extinction, with a finite wavenumber that in convective–diffusive scaling is proportional to the cube root of the Zel'dovich number. The convective–diffusive response contributes to the stabilization of long-wavelength disturbances through positive excess enthalpies by which the flame becomes more resistant to instability, while the reaction-zone response provides stabilization of short-wavelength disturbances by transverse diffusion, within the reactive inner layer, which relaxes the perturbed scalar fields towards their unperturbed states. As quasi-steady extinction is approached, marginal stability arises first at an intermediate range between these two scalings. Parametric results for this bifurcation point are obtained through numerical solutions of the associated generalized eigenvalue problems. Comparisons with measured pattern dimensions for different sets of reactants and diluents reveal excellent qualitative agreement.

1. Introduction

Intrinsic instabilities of flames arise from many sources, ranging from buoyancy (Taylor 1950) and hydrodynamics (Darrieus 1938; Landau 1944) to diffusional–thermal effects (Turing 1952; Sivashinsky 1977). Except for buoyancy, the known mechanisms of these instabilities apply specifically to premixed flames and are absent in diffusion flames, which exhibit fewer types of instability experimentally as well. Non-planar diffusional–thermal instabilities in particular, which arise through effects of diffusion of reactants and of thermal energy in the presence of finite-rate chemistry, as yet have been derived theoretically only for premixed flames. Among the many

† Present address: Environment Research Center, Korea Institute of Science and Technology, PO Box 131, Cheongryang, Seoul, 130-650 Korea.

premixed-flame analyses of diffusional–thermal instabilities are the early work of Barenblatt, Zel'dovich & Istratov (1962), the demonstration by Sivashinsky (1977) that cellular-flame instability occurs if the diffusivity of the limiting reactant is sufficiently larger than the thermal diffusivity, and the discovery by Joulin & Clavin (1979) of oscillatory instabilities as well when the diffusivity of the limiting reactant is sufficiently small compared with the thermal diffusivity. Clavin (1985) offers a comprehensive review of premixed-flame instabilities.

The present paper concerns the theory of cellular-flame types of instabilities for diffusion flames, some of which have been observed experimentally. As Buckmaster (1992) has pointed out, most reports of diffusion-flame instabilities, such as a number of observations related to ceiling fires, correspond to conditions under which buoyancy is significant. However, there are a few experiments (Garside & Jackson 1953; Dongworth & Melvin 1976; Ishizuka & Tsuji 1981; Chen, Mitchell & Ronney 1992) in which diffusion-flame instabilities have been reported for conditions under which buoyancy appears to be negligible. Ishizuka & Tsuji (1981) found that, when hydrogen, injected through the walls of a horizontal porous cylinder in a vertically flowing air stream, is sufficiently diluted with nitrogen or argon (but not with helium) the diffusion-flame sheet that is normally wrapped around the cylinder breaks up into flame stripes, leaving regularly spaced regions along the cylinder axis in which the combustion is extinguished. Dongworth & Melvin (1976) and Chen *et al.* (1992) studied instead Wolfhard–Parker types of burner configurations and under a variety of conditions found cellular-type patterns in the diffusion-flame sheet where fuel and oxidizer meet, especially near the base of the sheet. In all of these experiments, the spatial direction in which the periodicity occurs is the unstrained cross-stream direction; a rate of strain, that is 'stretch', in the periodicity direction tends to be stabilizing. The patterns observed in these experiments appear to arise from diffusional–thermal instabilities, and the present paper offers a theoretical analysis of a model problem designed to shed light on the mechanisms by which such instabilities may develop.

The patterns are observed experimentally for conditions under which the Lewis number of the fuel is less than unity, that is, the diffusion coefficient of the fuel in the fuel-inert stream is greater than the thermal diffusivity. By diffusion-flame symmetry, a Lewis number less than unity for the oxidizer in the oxidizer-inert stream also should favour the pattern formation. For these reasons, the present paper is restricted to Lewis numbers less than unity. Expansions for Lewis numbers near unity are not employed, and in that sense, in terminology applied to premixed flames (Buckmaster & Ludford 1982), the present approach resembles that for slowly varying flames rather than nearly equidiffusional flames. The method of analysis also applies to Lewis numbers greater than unity and in fact yields non-trivial results under these conditions as well, but to minimize complexity in exposition and to focus on conditions most directly applicable to existing experiments, presentation of results for Lewis numbers greater than unity will be postponed. Figure 1 is a schematic diagram of the type of pattern envisioned here as arising from the instability for Lewis numbers less than unity. Basically, the high-diffusivity reactants diffuse preferentially to the sinks provided by the strong segments of the reaction sheet, leaving the regions between deficient in reactants and therefore subject to local quenching.

The unperturbed flow configurations in the experiments described above are two-dimensional. The forward stagnation region of Ishizuka & Tsuji (1981), which controls the pattern formation, is approximated well by a counterflow diffusion flame, while the Wolfhard–Parker flows more closely resemble evolving mixing layers. In the present

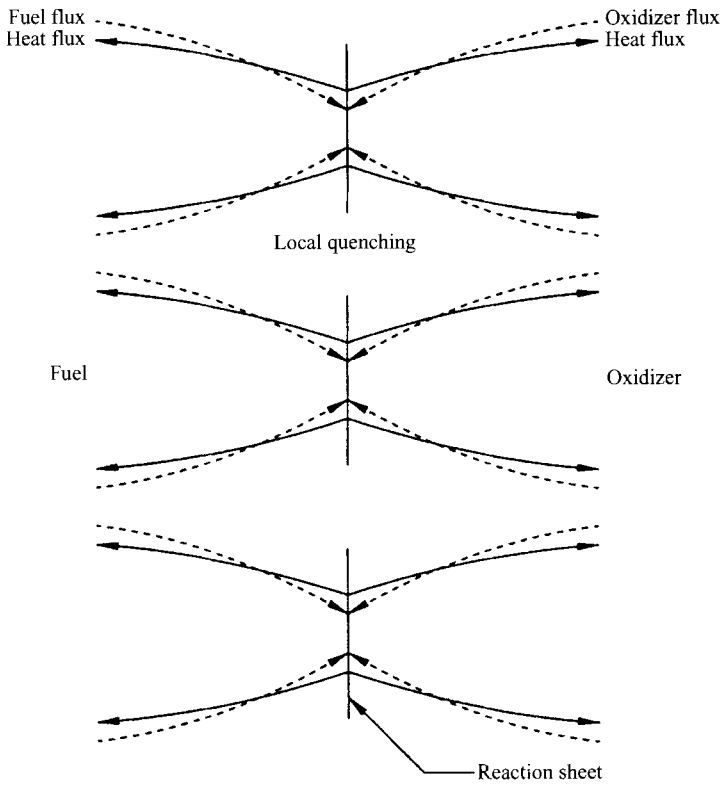

FIGURE 1. Schematic diagram of the diffusional–thermal instability of diffusion flame.

work, for simplicity the unperturbed flow is taken to be the one-dimensional convective diffusion flame illustrated in figure 2. In this configuration, there is a constant net mass flux, directed from the porous fuel plate toward the porous oxidizer plate, and fuel and oxidizer diffuse from their respective supply plates to the reaction sheet where they react to release thermal energy. At each porous plate the concentration of the species supplied is maintained constant. Convection is included here, rather than focusing on the simpler problem of a stagnant diffusion layer, because it is found from the analysis that convection is essential for instability to occur.

For the diffusion flame in a one-step Arrhenius approximation of reasonably high activation energy, stability in the flow configuration adopted here for one-dimensional time-dependent perturbations was analysed numerically quite a while ago by Kirkby & Schmitz (1966), who found interesting differences in behaviour for Lewis numbers less than and greater than unity. Their results are useful for testing the predictions of the present analysis qualitatively in the limit of large wavelengths of disturbance. The present theory can be considered to extend the analysis of Kirkby & Schmitz (1966) by addressing two-dimensional time-dependent perturbations, with periodicity imposed in the y-direction in figure 2, while maintaining complete uniformity in the third direction. These two-dimensional disturbances are introduced for the purpose of investigating the inception of the two-dimensional patterns seen in the experiments. Given the results to be developed here, it will be straightforward to analyse the corresponding instabilities of counterflow diffusion flames with cross-stream periodicity, for example; the only difference is that certain functions that arise in the analysis become more

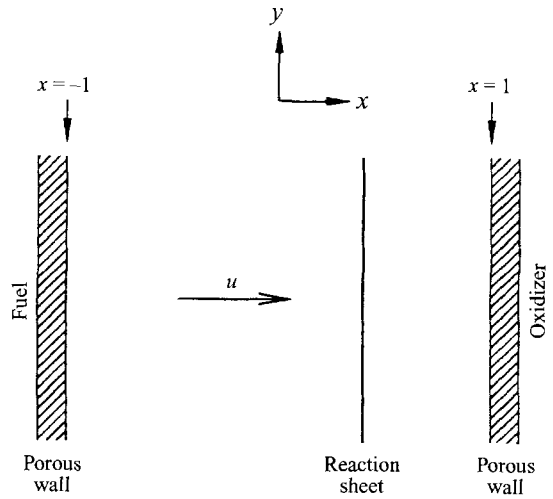

FIGURE 2. Schematic diagram of a one-dimensional convective–diffusion flame.

complicated for the counterflow. The model problem investigated here has thus been selected to be the simplest one possible that still illustrates the phenomena of interest.

The analysis to be presented here treats one-step, Arrhenius chemical processes with the Zel'dovich number β (a measure of the ratio of the activation energy to the thermal energy) taken to be a large perturbation parameter. The approach thus involves activation-energy asymptotics. For large β there are two distinct regimes of diffusion-flame structure (Liñán 1974): a premixed-flame regime, in which non-dimensional reactant concentrations in the reaction zone are of order β^{-1} for one reactant and unity for the other, and a diffusion-flame regime in which both non-dimensional reactant concentrations in the reaction zone are of order β^{-1}. When both boundary temperatures are well below the adiabatic flame temperature, as applies in the laboratory experiments identified above, the diffusion-flame regime can be relevant for nearly all values of the stoichiometric mixture fraction, while the premixed-flame regime can apply only for stoichiometric mixture fractions near zero or unity, since that structure is intrinsically unstable unless the non-dimensional temperature gradient on one side of the reaction zone is of order β^{-1} or smaller (Peters 1978). Stability analyses for the convective–diffusion flame will differ in the two regimes. Even in the premixed-flame regime, the stability behaviour will differ from that of premixed flames because of the different transport-zone structures, but the stability for the premixed-flame regime may be expected to resemble that for premixed flames more closely than would the stability for the diffusion-flame regime. Because of the known diffusional–thermal premixed-flame instabilities, this tends to suggest that the premixed-flame regime will be more relevant to the experimentally observed patterns. However, the same patterns are also seen for stoichiometric mixture fractions too far from the extremes for the premixed-flame regime to constitute the better of the two descriptions. Therefore, in the present paper attention is focused exclusively on the diffusion-flame regime. Future work will address the diffusion-flame stability for the premixed-flame regime, which in fact proves to be a simpler problem to analyse.

Attention initially will be devoted to perturbation frequencies and wavelengths of the same order as the corresponding time and length scales of the convective–

diffusive transport zones in the diffusion flame. For large β, the reaction-zone scales are shorter, and therefore the reactive–diffusive zone is treated as planar and quasi-steady in this initial analysis. It will be found that diffusion-flame instability can already arise with this scaling, but when it does there is always a divergence in the growth rate with decreasing scales. This divergence dictates the need to consider the next distinguished limit, which occurs at shorter scales, where unsteady and transversely varying disturbances arise within the reaction zone. The analysis for these shorter scales, the reaction-zone scales treated by Peters (1978), Stewart (1986) and Stewart & Buckmaster (1986) for the premixed-flame regime and by Buckmaster, Nachman & Taliafero (1983) for the diffusion-flame regime with Lewis number of unity, always provides stability at sufficiently short wavelengths. A composite expansion can be constructed from the results of the two distinguished analyses that yields a dispersion relation valid over the entire range of length scales. The general conclusions concerning the stability behaviour are drawn from this composite dispersion relation.

2. Formulation

The adopted configuration, illustrated in figure 2, is the same as that selected by Law & Chung (1982) for their analytical studies of Lewis-number effects in diffusion flames with infinite-rate chemistry. With ℓ denoting half the separation distance between the porous plates and D_T the thermal diffusivity, assumed constant for simplicity, characteristic length and time scales for diffusion may be taken to be ℓ and ℓ^2/D_T. These scales are used to construct the non-dimensional space (x, y) and time (t) coordinates, the x-coordinate being centred so that the walls are located at $x = \pm 1$, as indicated in figure 2. The uniform mass flux (m) in the $+x$-direction gives rise to a constant velocity m/ρ in that direction after introduction of the further assumption, also made for simplicity, that the density (ρ) is constant. The non-dimensional constant convection velocity is defined as $u = (m\ell)/(2\rho D_T)$. The diffusion coefficient is taken to be constant, as well as equal for both fuel and oxidizer, to avoid the complication of having to introduce an additional parameter, and the Lewis number $L \leqslant 1$ is the ratio of D_T to this diffusion coefficient. In terms of the heat release per unit mass of oxidizer consumed (Q) and the specific heat at constant pressure (c_p), assumed constant, a characteristic temperature is defined as $(QY_{O_1})/(c_pL)$, where Y_{O_1} denotes the oxidizer mass fraction at the oxidizer boundary. The non-dimensional temperature (T) is selected to be the temperature divided by this characteristic temperature, in which L has been included to facilitate describing the superadiabatic flame temperatures encountered in stagnant mixing layers when $L < 1$. The scaled oxidizer mass fraction (Y_O) is the oxidizer mass fraction divided by Y_{O_1}, and the scaled fuel mass fraction (Y_F) is the fuel mass fraction divided by νY_{O_1}, where ν denotes the stoichiometric mass ratio of fuel to oxidizer. A parameter that then appears in the boundary conditions is $A_F = Y_{F_{-1}}/(\nu Y_{O_1})$, where $Y_{F_{-1}}$ is the imposed fuel mass fraction at the fuel plate.

In the Arrhenius reaction rate, taken to be of order n with respect to fuel and m with respect to oxidizer, two additional parameters arise. One is the non-dimensional activation temperature, $T_a = (E/R)(c_pL)/(QY_{O_1})$, where E is the activation energy and R the universal gas constant. The other is the Damköhler number $D = BL\ell^2\nu^n Y_{F_{-1}}^n Y_{O_1}^{m-1}/D_T$, where B is a suitably defined frequency factor, with units of reciprocal time, which can expressed in terms of the pre-exponential factor B' of the reaction-rate constant as $B = B'(\rho/W_F)^n(\rho/W_O)^{m-1}$, in which W represents

molecular weight. Here any temperature dependence of the pre-exponential factor has been absorbed into the Arrhenius exponential factor, so that the frequency factor B can be treated as constant. With

$$w = D\, Y_F^n\, Y_O^m \exp(-T_a/T), \tag{1}$$

the non-dimensional formulation is then

$$\frac{\partial T}{\partial t} + 2u\frac{\partial T}{\partial x} - \nabla^2 T = w, \tag{2}$$

$$L\frac{\partial Y_i}{\partial t} + 2Lu\frac{\partial Y_i}{\partial x} - \nabla^2 Y_i = -w, \quad \text{for } i = O, F, \tag{3}$$

subject to

$$\left.\begin{aligned} T = T_F, \quad Y_F = A_F, \quad Y_O = 0, \\ T = T_O, \quad Y_F = 0, \quad Y_O = 1, \end{aligned}\right\} \tag{4}$$

Although u is constant here, it is equally possible to let u vary appropriately with x and impose conditions at $x = \pm\infty$, to describe the counterflow flame.

3. Forms of solutions in the convective–diffusive zones

According to activation-energy asymptotics, there are two convective–diffusive zones separated by a thin reaction zone. The source term w is negligible in the convective–diffusive zones at all algebraic orders in the small expansion parameter β^{-1}, but this term needs to be retained in all orders in the narrow reaction zone, the analysis of which provides jump conditions across the reaction sheet that serve as boundary conditions for the analysis of the convective–diffusive zones. In the convective–diffusive zones, solutions are sought in the form

$$\left.\begin{aligned} T &= \bar{T}(x) + \beta^{-1}\Phi(x) + \beta^{-1}\epsilon\varphi(x)\exp(iky + \sigma t), \\ Y_i &= \bar{Y}_i(x) + \beta^{-1}\Phi_i(x) + \beta^{-1}\epsilon\varphi_i(x)\exp(iky + \sigma t), \quad i = F, O, \end{aligned}\right\} \tag{5}$$

where $\beta = T_a/T_f^2$ is the Zel'dovich number, ϵ is the small perturbation parameter for the instability, k is the non-dimensional wavenumber, and σ is the non-dimensional growth rate, real parts of complex variables being understood to represent the physical quantities. In (5), $\bar{T}$ and $\bar{Y}_i$ represent the classical Burke–Schumann solutions that apply with infinite-rate chemistry and no reactant leakage. In addition to the instability perturbation functions φ and φ_i, it is found necessary to consider the leading steady-state Zel'dovich-number corrections Φ and Φ_i in the analysis of the convective–diffusive zones.

For the Burke–Schumann limit of infinite-rate chemistry, the steady-state outer solutions become

$$\bar{Y}_F = \begin{cases} A_F(1 - F_0^-) \\ 0, \end{cases} \quad \bar{Y}_O = \begin{cases} 0 \\ 1 - F_0^+, \end{cases} \quad \bar{T} = \begin{cases} T_F + (T_f - T_F)\,G_0^- \\ T_O + (T_f - T_O)\,G_0^+, \end{cases} \quad \begin{cases} -1 \leqslant x < x_f \\ x_f < x \leqslant 1, \end{cases} \tag{6}$$

where

$$F_0^{\pm} = \frac{\exp(Lux)\,\sinh[Lu(1 \mp x)]}{\exp(Lux_f)\,\sinh[Lu(1 \mp x_f)]}, \quad G_0^{\pm} = \frac{\exp(ux)\,\sinh[u(1 \mp x)]}{\exp(ux_f)\,\sinh[u(1 \mp x_f)]}. \tag{7}$$

Comparison of (6) and (21) below will show that an alternative to the first of these expressions is $F_0^{\pm} = (1 + A_F)(\mathrm{e}^{2Lux} - \mathrm{e}^{\pm 2Lu})/[A_F\,\mathrm{e}^{2Lu} + \mathrm{e}^{-2Lu} - (1 + A_F)\,\mathrm{e}^{\pm 2Lu}]$. Values

of x_f and T_f are determined by the jump conditions, which yield $\coth[Lu(1-x_f)] - A_F \coth[Lu(1+x_f)] = 1 + A_F$, giving

$$x_f = \frac{1}{2Lu} \ln\left[\frac{A_F\, e^{2Lu} + e^{-2Lu}}{1 + A_F}\right], \tag{8}$$

and

$$(T_f - T_O)\{\coth[u(1-x_f)]-1\} + (T_f - T_F)\{\coth[u(1+x_f)]+1\} = L\{\coth[Lu(1-x_f)]-1\}. \tag{9}$$

For the problem that is symmetric under convection-free conditions, $A_F = 1$ and $T_F = T_O = T_0$, expansions of the last two equations for small values of u give

$$x_f = Lu\left[1 - \left(\tfrac{2}{3}\right)(Lu)^2 + \cdots\right], \quad T_f = T_0 + \tfrac{1}{2}\left[1 - \left(\tfrac{1}{3}\right)(1-L^2)u^2 + \cdots\right]. \tag{10}$$

Corresponding expansions in (7) for x near x_f produce

$$F_0^{\pm} = 1 \mp (x - x_f) + \cdots, \quad G_0^{\pm} = 1 \mp (x - x_f) + u(1-L)(x - x_f) + \cdots. \tag{11}$$

In the opposite limit of large u, $x_f \to 1 - \ln 2/(2Lu)$ and $T_f \to T_0 + L(1-2^{-1/L})$. Some of the results will be given only for this symmetric problem, which has seven parameters, two fewer than (1)–(4). In addition, the reaction orders m and n usually will be taken to be unity, reducing the number of parameters to five.

When (5) is substituted into (2)–(4) for the convective–diffusive zones and terms of like powers of the small parameters are collected, then it is found for the stability problem that

$$\frac{\partial^2 \varphi}{\partial x^2} - 2u\frac{\partial \varphi}{\partial x} = (\sigma + k^2)\varphi, \tag{12}$$

$$\frac{\partial^2 \varphi_i}{\partial x^2} - 2Lu\frac{\partial \varphi_i}{\partial x} = (L\sigma + k^2)\varphi_i, \quad \text{for } i = O, F, \tag{13}$$

with null boundary conditions at $x = \pm 1$ and suitable jump conditions at the reaction sheet. Similar equations apply for Φ and Φ_i, but with vanishing right-hand sides. With the definitions $\Gamma = (L^2u^2 + L\sigma + k^2)^{1/2}$ and $\Gamma_0 = (u^2 + \sigma + k^2)^{1/2}$, the solutions to (12) and (13) are readily found to be $\varphi = a^{\pm}G_1^{\pm}$ and $\varphi_i = a_i^{\pm}F_1^{\pm}$, $i = F, O$, where $a^{\pm}$ and $a_i^{\pm}$ are coefficients of order unity, and

$$F_1^{\pm} = \frac{\exp(Lux)\sinh[\Gamma(1 \mp x)]}{\exp(Lux_f)\sinh[\Gamma(1 \mp x_f)]}, \quad G_1^{\pm} = \frac{\exp(ux)\sinh[\Gamma_0(1 \mp x)]}{\exp(ux_f)\sinh[\Gamma_0(1 \mp x_f)]}, \tag{14}$$

the superscript + applying for $x_f < x < 1$ and − for $-1 < x < x_f$. The steady-state perturbation solutions in the outer zones are similarly given by $\Phi = A^{\pm}G_0^{\pm}$ and $\Phi_i = A_i^{\pm}F_0^{\pm}$, with $F_0^{\pm}$ and $G_0^{\pm}$ defined in (7). Matching determines $a^{\pm}$, $a_i^{\pm}$, $A^{\pm}$ and $A_i^{\pm}$ from jump conditions in terms of reaction-zone coefficients. The analysis with convective–diffusive scaling centres on carefully defining the jump conditions.

4. The quasi-steady quasi-planar reaction zone

Jump conditions are obtained by analysing the inner reactive–diffusive layer using activation-energy asymptotics. The large parameter of expansion is β, and, with a normalizing adjustment factor defined as

$$f \equiv \frac{A_F Lu}{2}\{\coth[Lu(1+x_f)] + 1\} = \frac{Lu}{2}\{\coth[Lu(1-x_f)] - 1\}, \tag{15}$$

the stretched variables $\xi = \xi_f + \beta f(x - x_f)$, $\theta(\xi, y, t)$ and $\theta_i(\xi, y, t)$ are introduced, where $T = T_f - \beta^{-1}(\theta + \gamma\xi - \alpha)$ and $Y_i = \beta^{-1}\theta_i$, $i = F, O$, the values of the constants ξ_f, γ and α, of order unity, being selected to simplify the inner problem. These 'constants', like those below, could vary with y and t in the quasi-steady, quasi-planar description. Substitution into (1)–(3) yields, to leading order,

$$\frac{\partial^2\theta}{\partial\xi^2} = \frac{\partial^2\theta_F}{\partial\xi^2} = \frac{\partial^2\theta_O}{\partial\xi^2} = \Delta\,\theta_F^n\,\theta_O^m\,\mathrm{e}^{-(\theta+\gamma\xi)}, \tag{16}$$

where a reduced Damköhler number is defined as

$$\Delta \equiv Df^{-2}\,\beta^{-(1+m+n)}\,\mathrm{e}^{-T_a/T_f}\,\mathrm{e}^{\alpha}. \tag{17}$$

Matching slopes by use of (11) gives $\theta_F = \theta - \xi + \beta_F$, $\theta_O = \theta + \xi + \beta_O$ and $\partial\theta/\partial\xi \to \pm 1$ as $\xi \to \pm\infty$, if

$$\begin{aligned}\gamma \;=\; & \frac{\coth[u(1-x_f)] - \coth[u(1+x_f)] - 2}{\coth[u(1-x_f)] + \coth[u(1+x_f)]} \\ & + \frac{2\,(T_F - T_O)\,\{\coth[u(1-x_f)] - 1\}\,\{\coth[u(1+x_f)] + 1\}}{\{\coth[u(1-x_f)] + \coth[u(1+x_f)]\}\,\{Lu\coth[Lu(1-x_f)] - 1\}},\end{aligned} \tag{18}$$

so that, for $A_F = 1$ and $T_F = T_O = T_0$, $\gamma \to -(1 - L)u$ as $u \to 0$. The constants β_F and β_O, of order unity, may be set to zero by suitably selecting the values of ξ_f and α, which will then be determined from the forms of the outer solutions.

The resulting inner problem,

$$\left.\begin{aligned}\frac{\partial^2\theta}{\partial\xi^2} \;&=\; \Delta\,(\theta - \xi)^n\,(\theta + \xi)^m\,\mathrm{e}^{-(\theta+\gamma\xi)}, \\ \frac{\partial\theta}{\partial\xi} \;&\to\; \pm 1 \quad \text{as} \quad \xi \to \pm\infty,\end{aligned}\right\} \tag{19}$$

has been solved by Liñán (1974) for $m = n = 1$. His solution exhibits reactant leakage, defined by $\alpha_F = (\theta - \xi)|_{\xi\to\infty}$ and $\alpha_O = (\theta + \xi)|_{\xi\to-\infty}$, and demonstrates that, for each value of γ, the parameters α_F and α_O are functions of Δ. Figure 3 shows some of these leakage results for α_F, where it is seen that there is a minimum value of Δ below which no solution exists, the solution for α_F (and α_O) being double-valued when Δ is above this minimum. Figure 3 is for $\gamma \geqslant 0$, but the problem is symmetric in γ in that, for example, figure 3 applies for negative γ if α_F is replaced by α_O; typically γ is negative if $L < 1$ and $u > 0$, the case to be considered here, although the present analysis is equally applicable when u is negative. Appendix A provides further details on how the curves in figure 3 are computed.

For deriving the matching conditions for the solutions to (12) and (13), it is convenient to express the reaction-zone solutions as $\theta = \Theta(\xi) + \epsilon\,[\exp(\mathrm{i}ky + \sigma t)]\psi(\xi)$ and $\theta_i = \Theta_i(\xi) + \epsilon\,[\exp(\mathrm{i}ky + \sigma t)]\psi_i(\xi)$, to conform with the form of the expansion that has been adopted for the outer zones. Superscripts 0 will be placed on α, α_i and ξ_f to identify the steady-state parts, associated with Θ and Θ_i, which will be considered first, since the time-dependent parts can be treated quite analogously, but are more complicated algebraically.

Steady-state matching for temperature can be expressed as

$$T_f - \beta^{-1}(\Theta + \gamma\xi - \alpha^0) \;\sim\; T_f + \beta^{-1}[G_0'^{\pm}(T_f - T_0)(\xi - \xi_f^0)/f + A^{\pm}], \quad \xi \to \pm\infty, \tag{20}$$

through terms of order β^{-1}, where $G_0'^{\pm} \equiv (\mathrm{d}G_0^{\pm}/\mathrm{d}x)|_{x=x_f}$. The relationship between

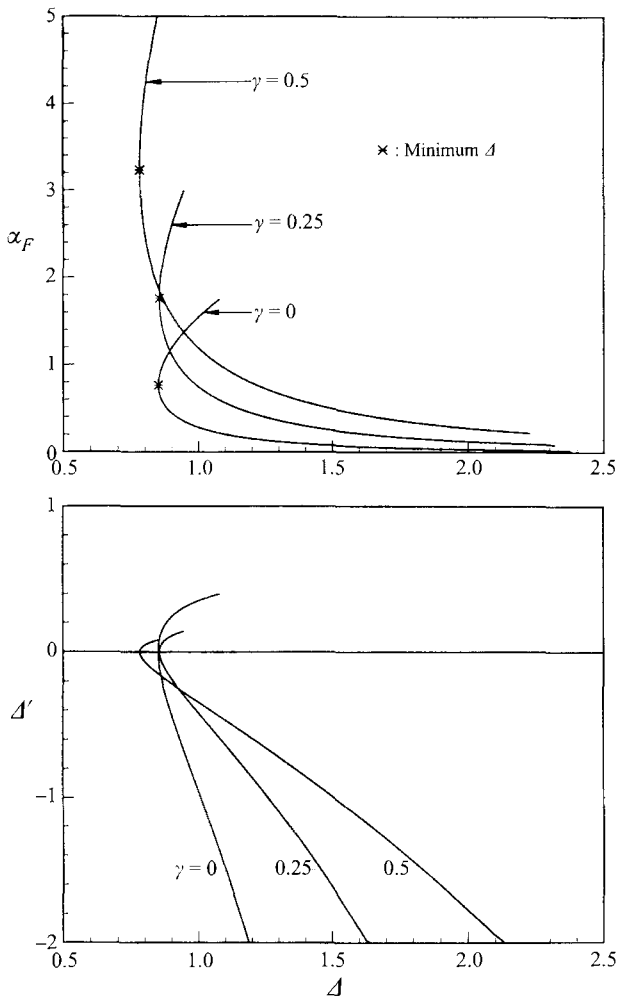

FIGURE 3. Variations of α_F and Δ' with Δ for $\gamma = 0$, 0.25 and 0.5.

x and ξ has been used here in the $G_0^{\prime\pm}$ terms so that the independent variables will be the same on both sides. Use of $\Theta \to \xi + \alpha_F^0$ as $\xi \to +\infty$ and $\Theta \to -\xi + \alpha_O^0$ as $\xi \to -\infty$ in (20) then provides relationships for $A^{\pm}$ in terms of α_F^0, α_O^0 and ξ_f^0, from the constant term of order β^{-1}. The term linear in ξ provides (9) and (18). Relations similar to (20) for Y_F and Y_O involve $F_0^{\prime\pm} = (\mathrm{d}F_0^{\pm}/\mathrm{d}x)|_{x=x_f}$ and similarly provide relationships for $A_F^{\pm}$ and $A_O^{\pm}$ in terms of α_F^0, α_O^0 and ξ_f^0; in particular $A_F^+ = \alpha_F^0$ and $A_O^- = \alpha_O^0$. Additional relationships come from the general coupling-function differential equations for $Y_F - Y_O$ and $T + Y_F$, which are independent of w. The former actually can be integrated exactly to show that

$$Y_O = Y_F + \frac{(1 + A_F)\,\mathrm{e}^{2Lux} - A_F\,\mathrm{e}^{2Lu} - \mathrm{e}^{-2Lu}}{\mathrm{e}^{2Lu} - \mathrm{e}^{-2Lu}}, \tag{21}$$

which in fact applies for the general unsteady problem as well, and it results in $A_F^+ = A_O^+$, $A_F^- = A_O^-$, and $\xi_f^0 = 0$. The last of these results enables one to deduce from (20) that $A^+ = \alpha^0 - \alpha_F^0$ and $A^- = \alpha^0 - \alpha_O^0$. The coupling equation for $T + Y_F$ shows

that $\mathrm{d}(T + Y_F)/\mathrm{d}x - 2uT - 2LuY_F$ is constant everywhere and, with the preceding relationships, results in

$$\alpha^0\{\coth[u(1-x_f)] + \coth[u(1+x_f)]\} = \alpha_F^0\{\coth[u(1-x_f)] - L\coth[Lu(1-x_f)]\}$$
$$+\alpha_O^0\{\coth[u(1+x_f)] - L\coth[Lu(1+x_f)]\} + (\alpha_F^0 - \alpha_O^0)(1-L). \qquad (22)$$

This last expression enables e^{α}, in (17) for Δ, to be related back to Δ itself, for the steady problem, by use of the results of the numerical solution to (19). This is the key final relationship that, for example, enables the quasi-steady extinction conditions to be calculated correctly.

A parallel development for the unsteady problem brings in the quantities $G_1'^{\pm} = (\mathrm{d}G_1^{\pm}/\mathrm{d}x)|_{x=x_f}$ and $F_1'^{\pm} = (\mathrm{d}F_1^{\pm}/\mathrm{d}x)|_{x=x_f}$, for example, $F_1'^{\pm} = Lu \mp \Gamma\coth[\Gamma(1\mp x_f)]$, and, with α^1 and α_i^1 referring to properties of ψ and ψ_i that correspond to α and α_i, it is again found that $a_F^+ = a_O^+ = \alpha_F^1$, $a_F^- = a_O^- = \alpha_O^1$, $\xi_f^1 = 0$, $a^+ = \alpha^1 - \alpha_F^1$, $a^- = \alpha^1 - \alpha_O^1$, and

$$\alpha^1\{\coth[\Gamma_0(1-x_f)] + \coth[\Gamma_0(1+x_f)]\}$$
$$= \alpha_F^1\{\coth[\Gamma_0(1-x_f)] - (\Gamma/\Gamma_0)\coth[\Gamma(1-x_f)]\}$$
$$+ \alpha_O^1\{\coth[\Gamma_0(1+x_f)] - (\Gamma/\Gamma_0)\coth[\Gamma(1+x_f)]\} + (\alpha_F^1 - \alpha_O^1)(1-L)u/\Gamma_0, \qquad (23)$$

where $\alpha = \alpha^0 + \epsilon[\exp(iky + \sigma t)]\alpha^1$, etc. In view of (17), it may be seen that α can be interpreted as a non-dimensional excess enthalpy at the reaction sheet, associated with the finite-rate chemistry for $u \neq 0$ and $L \neq 1$. That is, if $u = 0$ then there is an excess or deficiency of enthalpy at the Burke–Schumann flame, depending on whether $L < 1$ or $L > 1$, respectively, as a consequence of T_f corresponding to flame temperatures above or below the adiabatic flame temperature. When $u \neq 0$ and $L \neq 1$ this difference is reduced in accordance with (9) or (10), but the finite-rate chemistry causes an additional change if $u \neq 0$ and $L \neq 1$, associated with the factor e^{α} in the definition of Δ in (17). If either $u = 0$ or $L = 1$, then $\alpha = 0$. For brevity, henceforth α will be called simply excess enthalpy, although that term should be understood in the context just explained, that is, as an effect of finite-rate chemistry for $u \neq 0$ and $L \neq 1$.

5. Instability under convective–diffusive scaling

Although (22) can be used to extend and correct the diffusion-flame extinction analyses of Chung & Law (1983) and of Seshadri & Treviño (1989) with respect to Lewis-number effects, this aspect will be pursued elsewhere, where $L > 1$ is considered as well. Here attention is restricted to the instability for $L < 1$. From the definition of Δ and the inner-structure solution, it may be seen that (23) provides a dispersion relation for the stability problem. In particular, if $\Delta' \equiv \mathrm{d}\ln\Delta/\mathrm{d}\alpha_F$ and $r \equiv \mathrm{d}\alpha_O/\mathrm{d}\alpha_F$, then from the constancy of all other factors in the definition of Δ in (17), the combination $\Delta\mathrm{e}^{-\alpha}$ must remain constant, so that the perturbations must obey the equation

$$\Delta' = \Big[\{\coth[\Gamma_0(1-x_f)] - (\Gamma/\Gamma_0)\coth[\Gamma(1-x_f)]\}$$
$$+r\{\coth[\Gamma_0(1+x_f)] - (\Gamma/\Gamma_0)\coth[\Gamma(1+x_f)]\} + (1-r)(1-L)u/\Gamma_0\Big]$$
$$\times\Big\{\coth[\Gamma_0(1-x_f)] + \coth[\Gamma_0(1+x_f)]\Big\}^{-1}, \qquad (24)$$

derived by differentiating (23). Its transcendental nature causes (24) to be a rather complicated dispersion relation. However, its characteristics can readily be determined through expansions and numerical computations.

The Burke–Schumann limit of infinite reaction rate is that for which $\Delta \to \infty$, so that the only variations are those associated with the convective and diffusive processes. From figure 3 it is seen that in this limit $\alpha_F \to 0$, $\alpha_O \to 0$ and $\Delta' \to -\infty$. Equation (24) then reduces to $\coth[\Gamma_0(1-x_f)]+\coth[\Gamma_0(1+x_f)] = 0$, which also can be written as $\sigma = -k^2 - u^2 - N^2\pi^2/4$, where N denotes any integer. Since the largest value of σ, which corresponds to $N = 0$, is seen from this result to be negative for all values of k, the Burke–Schumann solution is found to be stable for all wavelengths. The leakage effects associated with finite values of Δ' thus must be addressed to investigate the possibility of instability.

It is first worth remarking that the ordinary quasi-steady extinction condition corresponds to the minimum value of the Damköhler number D for which a solution exists. In view of the definition of Δ, this minimum coincides with the minimum of $\Delta e^{-\alpha}$, that is, the minimum of $\ln\Delta - \alpha$, not simply the minimum of $\ln\Delta$. The condition for this minimum to occur can be expressed as $\Delta' = d\alpha/d\alpha_F$, this last derivative being obtained from (22) and being given by (24) with $\sigma = k = 0$. If either $u = 0$ or $L = 1$, then $d\alpha/d\alpha_F = 0$, since the quasi-steady excess enthalpy vanishes, $\alpha^0 = 0$, and the minimum value of D coincides with the minimum of Δ. In this case, the upper branch of the S-curve for the maximum temperature as a function of the Damköhler number ranges over $-\infty \leqslant \Delta' \leqslant 0$, and interest centres mainly on negative values of Δ'. If, however, $d\alpha/d\alpha_F > 0$, then the ordinary quasi-steady extinction evidently occurs at a positive value of Δ', and there is interest in values of Δ' extending at least from $-\infty$ up to this positive value. In this situation, as α_F increases, the product $\Delta e^{-\alpha}$ continues to decrease for a while even after Δ begins to increase, because of the continuing increase in the excess enthalpy α. This situation is indeed often encountered when $u \neq 0$ and $L < 1$, the conditions addressed here. Therefore, it is important to consider not only negative values of Δ' but also a range of positive values. The positive value that Δ' achieves at the ordinary quasi-steady extinction condition will be termed here simply the extinction value, for brevity, even though stability analyses of the kind being pursued here are needed for ascertaining whether this quasi-steady turning point does indeed coincide with extinction.

The planar instability, studied numerically by Kirkby & Schmitz (1966), is recovered from the present approach by putting $k = 0$. From preceding results it is seen that, in the Burke–Schumann limit, the growth rate for planar disturbance is $\sigma = -u^2 - N^2\pi^2/4$, always negative, implying stability. As Δ' increases, this result changes. The expansion of (24) for small values of Γ and Γ_0 with $A_F = 1$ and $T_F = T_O = T_0$ can be investigated to get an idea of how the change occurs. To derive this expansion it is necessary to retain two terms, $\coth x = x^{-1}(1 + x^2/3 + \cdots)$, and to use the fact that, excluding possible uninteresting stable situations in which σ is negative and not small, when Γ_0 is small, u^2 (and k^2) must also be small, so that, from (10), x_f also is small. The result of the expansion then turns out to be simply

$$\sigma\,[(1-L)(1+r) - 2\Delta'] = 6\Delta' - (1-L^2)(1+r)u^2 - 3(1-L)(1-r)u, \qquad (25)$$

which applies only for small values of σ. Equation (25) is inconsistent with the Burke–Schumann limit because in that limit $\Gamma_0 = N\pi i/2$, which is not small unless $N = 0$, and even for $N = 0$ the limit is approached through values of Γ_0 of order unity, inconsistent with (25), which has treated Δ' as being of order unity, not large. Nevertheless, (25) retains the qualitatively correct behaviour that σ becomes negative

($\sigma \to -3$) as $\Delta' \to -\infty$. Equation (25) shows that σ increases as Δ' increases, passing at $\Delta' = 0$ through the small value $-[(1+L)u^2 + 3u(1-r)/(1+r)]$, negative unless r is sufficiently large, and reaches zero at $\Delta' = (1-L^2)(1+r)u^2/6 + (1-L)(1-r)u/2$, often a positive value. For small values of u, this value of Δ' is the extinction value, defined above, since the planar instability problem with $\sigma = 0$ (marginal planar instability) is the same as the quasi-steady extinction problem. With further increases of Δ', (25) shows σ to increase through positive values, approaching infinity at $\Delta' = (1-L)(1+r)/2$, a value that (for $L < 1$) always exceeds that for which $\sigma = 0$, the ratio of the two values being $(1+L)u^2/3 + u(1-r)/(1+r)$, and u being small. Of course, with small Γ_0, results from (25) are restricted to small values of σ, and in any event the stability results can describe the behaviour of the perturbed system for all time only up to the bifurcation, $\sigma = 0$.

In general, u is not small, and investigation of the planar instability then involves numerical solution of (24) with $k = 0$. The numerical solutions exhibit qualitatively the same type of character that was deduced from (25). Values of σ are always real, and they are negative for Δ' sufficiently negative and increase with Δ', reaching zero at a finite value of Δ'. The results agree quantitatively with (25) when u and σ are sufficiently small. They also are qualitatively consistent with those of Kirkby & Schmitz (1966), but quantitative comparisons are not possible because the precise bifurcation conditions which can be related to Δ' were not presented in that early study.

Non-planar instabilities are studied by considering $k \neq 0$ in (24). It is evident at the outset, from the present results, that there is no distinguished limit for small values of k. Values of σ from the dispersion relation vary smoothly with k for values of k that are small or of order unity. This smooth variation must be calculated numerically from (24), and representative results are shown by the solid curves in figure 4 for various values of Δ', with $r = 1$, $L = 0.4$ and $u = 1$. The maximum value of Δ' in the figure is the extinction value. It is seen from figure 4 that the system remains stable for all values of k if $\Delta' \leqslant 0$, and the decay rate of any disturbance increases with increasing k when $\Delta' < 0$, so that the least-stable disturbance is the planar one, although the system is stable to this planar disturbance as well. However, for $\Delta' > 0$, the situation is reversed, in that the shorter the wavelength of the disturbance is, the less stable the system is, and there always exists a wavelength below which instability is predicted. This instability in coordinates scaled by the convective–diffusive zones suggests that $\Delta' = 0$ is in fact the limiting value for the system, rather than the extinction value, and whenever $\Delta' > 0$ a non-planar instability with a wavelength shorter than this scale will occur. This result is the first finding of such a cellular type of instability for the diffusion flame and lends significance to the results of Chung & Law (1983), who treated $\Delta' = 0$ as an important critical value, even though they did not recognize that this value corresponds to the onset of cellular instability when $L < 1$.

The present findings for $k \neq 0$ motivate the investigation of different scaling at larger k that will apply in the vicinity of $\Delta' = 0$ and $\sigma = 0$, to find a stabilizing influence. Efforts to find such scaling revealed no distinguished limits other than that of the reaction-zone scaling, considered in the following sections. An appropriate procedure for addressing the cellular instability therefore is to study the implications of a stability analysis with reaction-zone scaling.

Asymptotic results for large k, obtained from the present scaling, are needed for properly interpreting results of the stability analysis with reaction-zone scaling. These asymptotic results also aid in identifying when cellular instability may arise. An

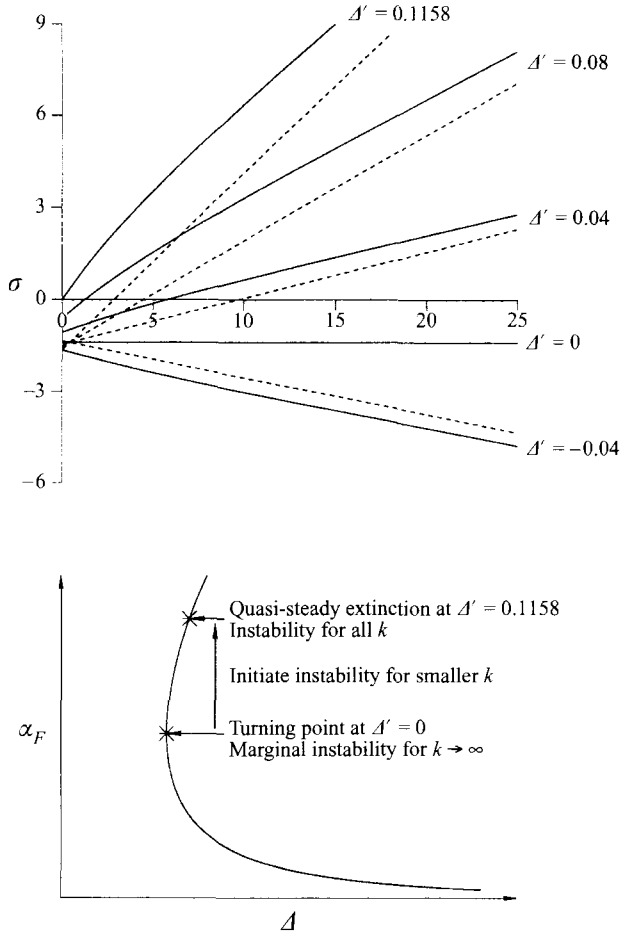

FIGURE 4. Dispersion relations obtained from the convective–diffusive scaling analysis for various values of Δ' with $r = 1$, $L = 0.4$ and $u = 1$. The largest value of Δ' corresponds to the steady-state extinction. Solid lines, dispersion relation; dashed lines, asymptote.

expansion of (24) for $k \to \infty$ provides these asymptotic results. As $k \to \infty$, both Γ and Γ_0 become large, and the hyperbolic cotangents all approach unity plus exponentially small terms. Equation (24) then reduces simply to the relationship $\Gamma_0[1 - 2\Delta'/(1+r)] = \Gamma - u(1-L)(1-r)/(1+r)$, the last term of which is a small correction when k is large. Omitting this term results in the expression

$$\sigma\left[\left(1-\frac{2\Delta'}{1+r}\right)^2 - L\right] = -u^2\left[\left(1-\frac{2\Delta'}{1+r}\right)^2 - L^2\right] + \frac{2\Delta'}{1+r}\left(2-\frac{2\Delta'}{1+r}\right)k^2, \quad (26)$$

which is plotted as the dashed lines in figure 4. The negative slope is evident for $\Delta' < 0$, while at $\Delta' = 0$ the constant value $\sigma = -(1+L)u^2$ is achieved, consistent with (24) and (25) for $r = 1$, in which special case the asymptotic result applies for all k and even gives the planar stability behaviour correctly. When Δ' becomes positive, (26) predicts instability for wavenumbers above the critical value

$$k = \left\{u^2\frac{1+r}{2\Delta'}\left[\left(1-\frac{2\Delta'}{1+r}\right)^2 - L^2\right]\left(2-\frac{2\Delta'}{1+r}\right)^{-1}\right\}^{1/2} \equiv k_c. \quad (27)$$

The growth rate σ of the instability actually is predicted to become infinite when Δ' reaches the value $(1 - L^{1/2})(1 + r)/2$, but the approximation needs to be restricted to small positive values of Δ' and must fail before this value is reached. Within their ranges of validity for positive Δ', (26) and (27) can be simplified to $\sigma = 4\Delta'(k^2 - k_c^2)/[(1 + r)(1 - L)]$ and $k_c^2 = u^2(1 - L^2)(1 + r)/(4\Delta')$. The last of these expressions provides a rough preliminary estimate of the transverse cell dimension of the instability, $2\pi/k_c$, dimensionally:

$$\ell_T = \frac{4\pi(\ell/u)\Delta'^{1/2}}{[(1+r)(1-L^2)]^{1/2}} = \frac{8\pi(\rho D_T/m)\Delta'^{1/2}}{[(1+r)(1-L^2)]^{1/2}}, \tag{28}$$

which is the ratio of the thermal diffusivity to the convective velocity multiplied by a factor that is proportional to the small quantity $\Delta'^{1/2}$. It will be seen below that for large β neutral stability is achieved at a particular (small) value of $\Delta'^{1/2}$, which is not determined by the present scaling.

6. Stability analysis with reaction-zone scaling

In reaction-zone scaling, $K = k/(\beta f)$ and $S = \sigma/(\beta f)^2$ are treated as being of order unity. To prevent unbalance of the transverse-derivative terms, the only outer solutions consistent with (12) and (13) and their boundary conditions at $x = \pm 1$ are then $\varphi = \varphi_i = 0$. The disturbances are confined to the reaction zone and must vanish as the reaction-zone spatial coordinate approaches $\pm\infty$. Expansions for the reaction zone are then introduced in the form indicated after (14),

$$\left.\begin{aligned} T &= T_f - \beta^{-1}[\Theta(\xi) + \gamma\xi - \alpha] + \beta^{-1}\epsilon\,[\exp(iky + \sigma t)]\,\psi(\xi), \\ Y_i &= \beta^{-1}\Theta_i(\xi) + \beta^{-1}\epsilon\,[\exp(iky + \sigma t)]\,\psi_i(\xi), \quad i = F, O, \end{aligned}\right\} \tag{29}$$

analogous to (5), and from (1)–(3) the differential equations for the time-dependent reaction-zone perturbations are derived, to leading order, as

$$\frac{d^2\psi}{d\xi^2} - (S + K^2)\psi = \frac{d^2\psi_F}{d\xi^2} - (LS + K^2)\psi_F = \frac{d^2\psi_O}{d\xi^2} - (LS + K^2)\psi_O$$

$$= \Delta(\Theta - \xi)^n(\Theta + \xi)^m e^{-(\Theta+\gamma\xi)}\left[\frac{n\psi_F}{\Theta - \xi} + \frac{m\psi_O}{\Theta + \xi} - \psi\right]. \tag{30}$$

Here $\Theta(\xi)$ is the solution to the problem defined by (19). Since the equation and the boundary conditions for ψ_F and ψ_O are identical as a consequence of the equal Lewis numbers of the two reactants, it follows that $\psi_F = \psi_O \equiv \chi(\xi)$, and then, for $m = n = 1$, (30) reduces to the pair of equations

$$\frac{d^2\psi}{d\xi^2} - (S + K^2)\psi = \frac{d^2\chi}{d\xi^2} - (LS + K^2)\chi = \Delta e^{-(\Theta+\gamma\xi)}[2\Theta\chi - (\Theta^2 - \xi^2)\psi], \tag{31}$$

subject to $\psi \to 0$ and $\chi \to 0$ as $\xi \to \pm\infty$, from matching. In (31), the terms involving S represent the time-dependent effects in the reaction zone, and the terms involving K^2 account for transverse diffusion in that zone, so that the reaction zone is neither planar nor quasi-steady any more. Because of the shorter time scale, instabilities found with this scaling often have been called fast-time instabilities.

For $L = 1$, (31) gives $\chi = \psi$, and a classical eigenvalue problem is obtained, with

'energy' $E = -(S + K^2)$ and 'potential' $V(\xi) = \Delta(2\Theta - \Theta^2 + \xi^2)e^{-(\Theta+\gamma\xi)}$, such that

$$\frac{d^2\psi}{d\xi^2} + (E - V)\psi = 0, \quad \psi(\pm\infty) = 0. \tag{32}$$

Since $V \to 0$ as $\xi \to \pm\infty$, it is known (cf. Titchmarsh 1946; Morse & Feshbach 1953) that there is a continuum of eigenvalues E for $E \geqslant 0$ and at most a discrete number of eigenvalues for $E < 0$. There are no discrete eigenvalues unless $V(\xi) < 0$ somewhere. Although $V(\xi) > 0$ if $|\xi|$ is sufficiently large, the solution to (19) has a range of ξ over which $V(\xi) < 0$; e.g. $\Theta(0) > 2$, for the branch of solutions $\Theta(\xi)$ that has the greater amount of leakage, that is, for $\Delta' > 0$. Therefore, negative eigenvalues exist for $\Delta' > 0$. These negative values of E correspond to instability ($S > 0$) at sufficiently small values of K. Interest centres on the least-stable solutions, that is, on the largest negative eigenvalues, and for these lowest energies, the eigenfunctions ψ have no zeros for finite values of ξ. For these solutions, $S = -E - K^2$ is maximum for $K = 0$ and negative for $K > (-E)^{1/2}$. Buckmaster *et al.* (1983) addressed this problem for $K = 0$ and concluded that the upper branch of the S-curve of the peak temperature as a function of the Damköhler number (the branch that approaches the Burke–Schumann limit) is stable, with instability setting in at the turning point, $\Delta' = 0$, the quasi-steady extinction point. This same conclusion clearly applies if transverse diffusion ($K \neq 0$) is permitted. The negative slope of the straight line of S as a function of K^2 demonstrates the stabilizing influence of transverse diffusion in the reaction zone. In contrast to the results for $L < 1$ with convective–diffusive scaling, stability now always is encountered at sufficiently large K.

For $L \neq 1$, the problem defined by (31) is a generalization of that defined by (32), and the solutions are of similar character. The equations were integrated numerically using a shooting method. The expansions for $\xi \to \pm\infty$,

$$\frac{d\psi}{d\xi} \to \mp(S + K^2)^{1/2}\psi, \quad \frac{d\chi}{d\xi} \to \mp(LS + K^2)^{1/2}\chi, \quad \text{as} \quad \xi \to \pm\infty, \tag{33}$$

were employed as the boundary conditions for the integrations. These conditions provide decay at infinity when the quantities inside the radicals are positive and oscillation at infinity when they are negative; the integrations were performed only when there was decay. The solutions ψ and χ were monitored to make sure that they did not vanish in the range of integration, so that the largest negative eigenvalue would be obtained. The procedure involved selecting values of K, L, Δ and γ and adjusting S until the boundary conditions were satisfied. Results for $S + K^2$ as a function of Δ' for $\gamma = 0$ are shown in figure 5, in which the curves for $L \neq 1$ correspond to $K = 0$. Growth rates are seen to increase with increasing Δ' and with increasing L. Positive values of S are obtained only for $\Delta' > (1 - L^{1/2})(1 + r)/2$. This onset condition is derived analytically in Appendix B. It may be noted that, for $L < 1$, the situation considered here, the onset of the fast-time instability at $K = 0$ does not occur until after the turning point, namely where the growth rate from (26), the asymptotic expression with convective–diffusive scaling, becomes infinite. Thus, the fast-time response is a stabilizing influence over a range of conditions for which the stability analysis with convective–diffusive scaling predicts instability.

A typical set of results for the dispersion relation, obtained numerically as just described, is shown in figure 6, in which $\gamma = 0$, $L = 0.4$ and Δ' ranges from 0 to $1 - L^{1/2}$. Although S does not exceed zero at $K = 0$ until $\Delta' > 1 - L^{1/2}$, it is seen in figure 6 that for $\Delta' > 0$ there is a range of values of K, between zero and a maximum value that is not very large, over which $S > 0$. Thus, whenever $\Delta' > 0$, the reaction-

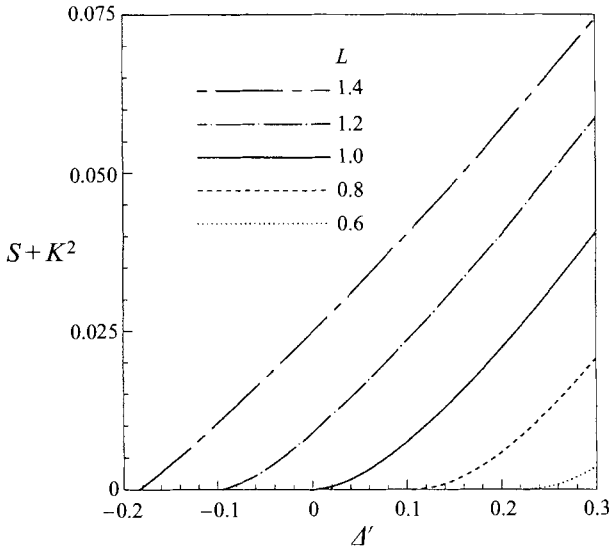

FIGURE 5. Variations of $S + K^2$ with Δ' for various values of L with $\gamma = 0$. The curves for $L \neq 1$ correspond to $K = 0$.

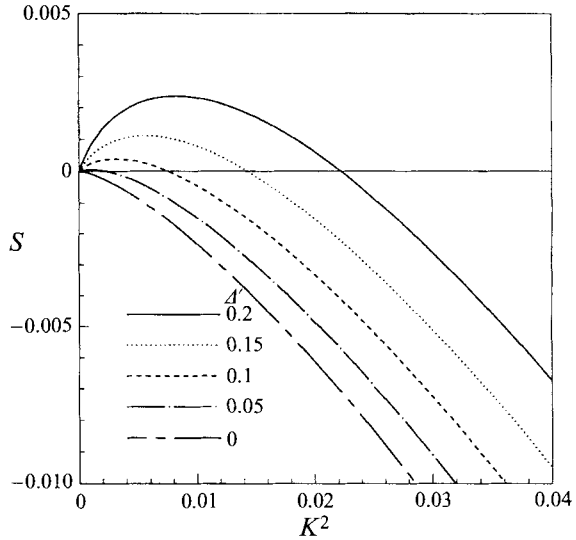

FIGURE 6. Variations of S with K^2 for various values of Δ' with $L = 0.4$ and $\gamma = 0$.

zone scaling predicts instability over some range of K. This result again points to the relevance of $\Delta' = 0$ as a critical value, despite the ever existing stabilization at large values of K. Since the instability is found here only for small values of K, further attention to the accuracy of the instability prediction with reaction-zone scaling is warranted. Such considerations are aided by expansions for small values of K and S.

Under conditions like those in figure 6, where $S = 0$ at $K = 0$, near $K = 0$ the growth rate S is found to be linear in K^2, namely $S = CK^2$. The constant of proportionality C can be obtained by a perturbation approach similar to that given

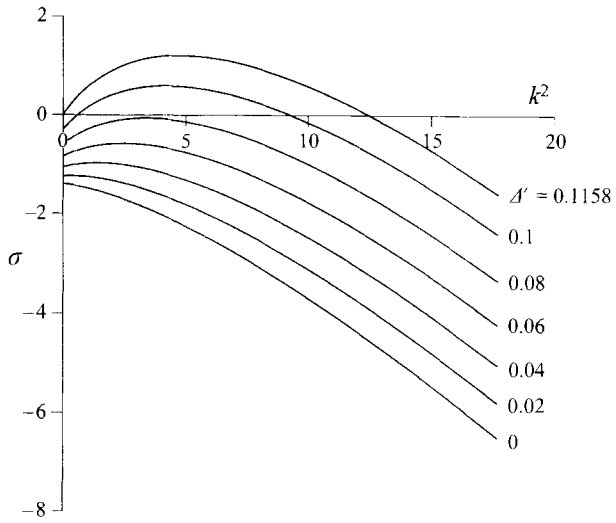

FIGURE 7. Dispersion relations obtained from composite expansions of the reaction-zone scaling analysis and convective–diffusive scaling analysis. $\beta = 10$, $\gamma = 0$, $u = 1.0$, $L = 0.4$.

in Appendix B. This analysis, outlined in Appendix C, results in

$$S = \frac{[2\Delta'/(1+r)]\,[2-2\Delta'/(1+r)]}{[1-2\Delta'/(1+r)]^2 - L}\,K^2, \tag{34}$$

which bears a striking resemblance to (26). This result provides a basis for combining the two analyses, in seeking uniformity, as shown in the following section.

7. The composite expansion of the dispersion relation

The results of the stability analyses with convective–diffusive and reaction-zone scalings can be combined by observing that the slope of the curve of σ as a function of k^2, obtained from (26), is the same as that obtained from (34). That is, this slope of the dispersion relation obtained with convective–diffusive scaling as $k \to \infty$ is the same as that obtained with reaction-zone scaling in the limit $K \to 0$. A composite expansion may therefore be considered, with the Zel'dovich number β the large parameter of expansion and the last term in (26) the common part. Let $\Sigma(k)$ denote the dispersion relation for σ obtained numerically with convective–diffusive scaling and $S(K)$ the dispersion relation for $\sigma/(\beta f)^2$ obtained numerically with reaction-zone scaling. Then a dispersion relation uniformly valid in k for large values of β is

$$\sigma = \Sigma(k) + (\beta f)^2 S(k/\beta f) - \frac{[2\Delta'/(1+r)]\,[2-2\Delta'/(1+r)]}{[1-2\Delta'/(1+r)]^2 - L}\,k^2. \tag{35}$$

Figure 7 illustrate the results of the uniform expansion, computed numerically, for a representative case. For the curve corresponding to $\Delta' = 0.1$ in figure 7, the inner (convective–diffusive) and outer (reaction-zone) scalings and the way they are combined are illustrated in figure 8.

As illustrated in figure 7, there is a range of parameters over which the system is stable for all values of k. However, as Δ' increases above zero, an intermediate range of k arises, over which instability is encountered. In figure 7, the marginal stability condition begins at about $\Delta' = 0.08$ and has a wavenumber k of about

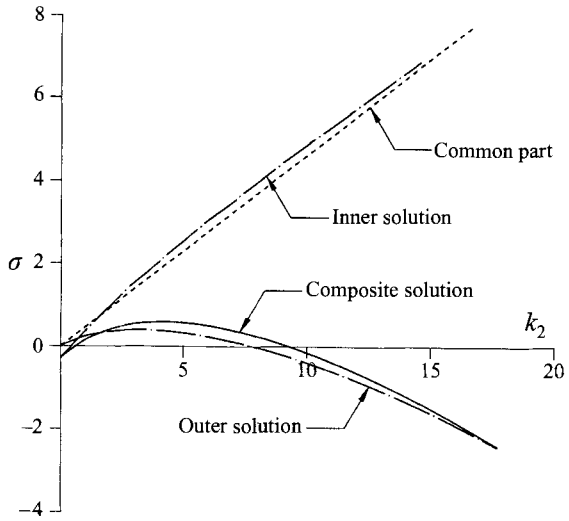

FIGURE 8. A representative illustration of the composite expansion of the reaction-zone scaling analysis and convective–diffusive scaling analysis for $\Delta' = 0.1$ with $L = 0.4$, $\gamma = 0$, $u = 1$ and $\beta = 10$.

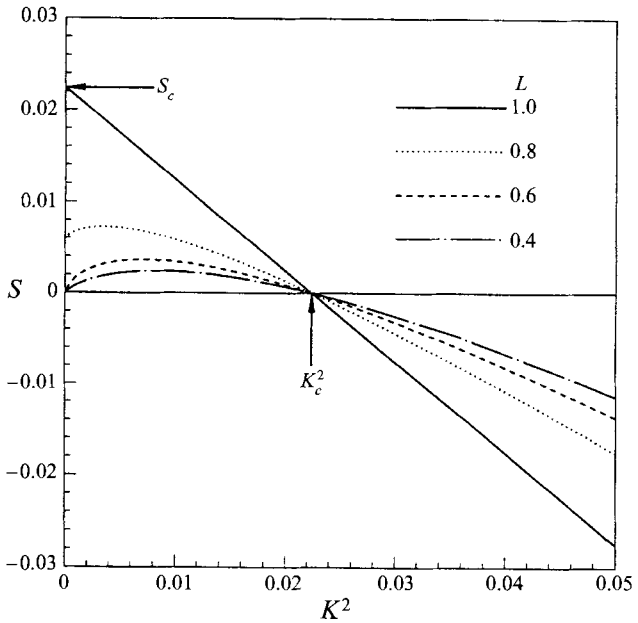

FIGURE 9. Variations of S with K^2 at a fixed value of Δ for various values of L.

2. When instability first arises it therefore does so at a finite transverse dimension, which should provide a good approximation to the transverse cell dimension observed experimentally and an improvement over (28). The numerical results indicate that the wavenumber of the fastest growing mode increases slightly with increasing Δ', but this change is small, so that the marginal stability condition should provide an excellent estimate of the transverse cell dimension.

It is noteworthy that, in figure 7, which corresponds to a realistic value of β, the

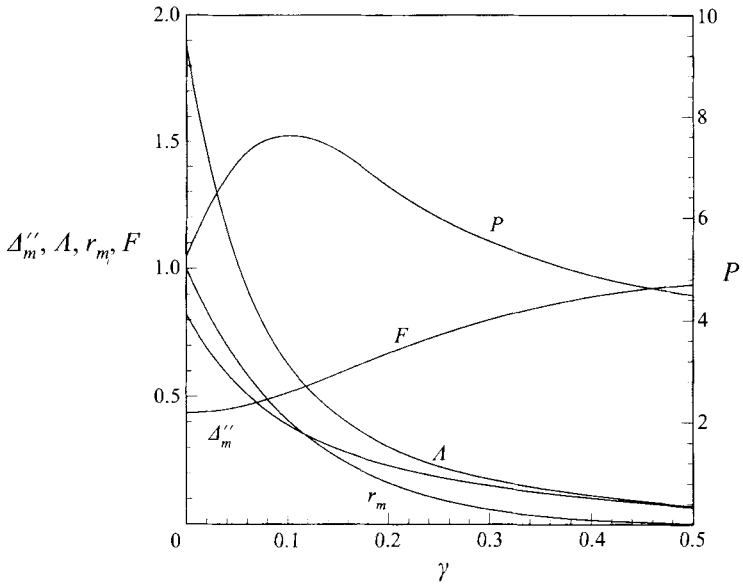

FIGURE 10. Variations of Δ''_m, Λ, r_m, P and $F = \Delta''_m(1+r_m^2)/[\Lambda(1+r_m)]$ with γ.

cell dimension has $k \approx 2$, a value roughly of order unity with the scaling of the convective–diffusive zone. This is in qualitative agreement with experiment. Reaction-zone scaling would give a transverse dimension that was too short. Thus, even though the reaction-zone scaling is needed for completing the analysis given here, the resulting cell size is predicted to be larger than this. Marginal stability is seen in figure 7 to begin at a value of Δ' greater than zero. The computations show that, as β becomes larger, the instability begins at smaller values of Δ', values that approach zero as β approaches infinity, and the value of k for marginal stability with convective–diffusive scaling approaches infinity as β approaches infinity. However, at reasonable values of β, this value of k is not large.

It is appropriate to seek simplification of these results for large β by introducing an expansion for small Δ' within the present expansion. The results with convective–diffusive scaling are summarized after (27). With reaction-zone scaling, to identify the value of K at which S is maximum, it is necessary to extend the analysis one term farther. In this context, it is of interest to note that in the reaction-zone analysis of the previous section, the value of K_c at which S returns to zero after becoming positive is independent of L when the values of the other parameters are fixed. This result is illustrated in figure 9, where S is plotted as a function of K^2 for various values of L with $\gamma = 0$ and $\Delta' = 0.2$; it is seen from this figure that K_c is independent of L, as suggested by (31), which is independent of L when $S = 0$, and it is found from the straight line for $L = 1$ that $K_c^2 = S_c$, the value of S for $K = 0$ and $L = 1$, given by the curve for $L = 1$ in figure 5.

To find K_c for small values of Δ', it is necessary to carry out a two-term expansion of (31), as summarized in Appendix C. When the expansion of the potential in (32) is considered near the minimum of Λ, it is found according to (C 12) that, for small values of Δ', $K_c^2 = P\Delta'^2$, where P is a constant of order unity and independent of L; figure 10 shows P as a function of γ. The expansion of (35) for small values of Δ'

then becomes, by use of (26) and (C 14),

$$\sigma = \frac{4\Delta'}{(1+r)(1-L)}\left[(k^2-k_c^2) - \frac{k^4}{\beta^2 f^2 P \Delta'^2}\right], \tag{36}$$

which with k_c defined by (27) is an explicit dispersion relation in terms of the slope $(1/\Delta')$ of the curve of the leakage as a function of the logarithm of the reduced Damköhler number for the unperturbed, steady-state problem.

If Δ' is sufficiently small, then (36) predicts stability for all k, that is $\sigma < 0$. At sufficiently large values of Δ', there are two values of k for which $\sigma = 0$ in (36), and the system is unstable for values of k between these two values. The marginal stability condition is that for which the equation obtained by substituting $\sigma = 0$ into (36) has only one solution. This occurs when

$$\Delta' = \frac{2k_c}{\beta f P^{1/2}} = \beta^{-2/3}\left[\frac{(1-L^2)(1+r)}{P(f/u)^2}\right]^{1/3}, \tag{37}$$

where use has been made of (27) in deriving the last equality, and the corresponding value of k is

$$k_T = u\beta^{1/3}\left[\frac{\Lambda(1+r_m)(f/u)(1-L^2)}{\sqrt{2}\,\Delta_m''(1+r_m^2)}\right]^{1/3}, \tag{38}$$

where the subscript m identifies conditions at the minimum value of the reduced Damköhler number, Λ is an eigenvalue-type integral, and Δ'' is Δ^{-1} times the curvature of the reduced Damköhler number with respect to fuel leakage. Here $(f/u) = A_F L\{\coth[Lu(1+x_f)]+1\}/2$ from (15), and, for the case $A_F = 1$, for example, $(f/u) \to 1/(2u)$ as $u \to 0$ and $(f/u) \to L$ as $u \to \infty$. Since the limit of large u is most relevant to the majority of experimental conditions (Ishizuka & Tsuji 1981; Chen *et al.* 1992), the factor (f/u) is usually found to be independent of u, so that the value of Δ' at marginal stability is only weakly dependent on u, through its influence on the values of P and r.

It is worthy of note that the $\beta^{-2/3}$ dependence of Δ' in (37) and the $\beta^{1/3}$ dependence of k_T in (38) come from the fact that k_c is inversely proportional to $\Delta'^{1/2}$. Equation (38) gives for the improved estimate of the transverse cell length

$$\ell_T = \frac{2\pi\ell}{u\beta^{1/3}}\left[\frac{\sqrt{2}\,F}{(f/u)(1-L^2)}\right]^{1/3} = \frac{4\pi\rho D_T}{m\beta^{1/3}}\left[\frac{\sqrt{2}\,F}{(f/u)(1-L^2)}\right]^{1/3}, \tag{39}$$

which is to be compared with (28). Here $F = \Delta_m''(1+r_m^2)/[\Lambda(1+r_m)]$, and figure 10 shows the parameters Λ, Δ_m'', r_m and F appearing here, as functions of γ. The estimate of ℓ_T given in (28) is not too bad in that, if (37) is substituted into (28), then the resulting value of ℓ_T exceeds that obtained from (39) only by a factor of $\sqrt{2}$. However, (28) is incomplete in that it does not provide a means for estimating the value of Δ' needed for marginal stability. In (39), ℓ_T is only weakly dependent on the small parameter of expansion, being proportional to $\beta^{-1/3}$, so that the stabilization of short wavelengths achieved through the behaviour with reaction-zone scaling does not strongly influence the final cell size.

The analysis with convective–diffusive scaling applied for arbitrary $L < 1$ and did not address simplification that may occur as the Lewis number approaches unity. Equation (38) suggests that is may be worthwhile to consider $1 - L$ of order β^{-1} with convective–diffusive scaling. In this limit, k_T is of order unity, and marginal

stability may be found at a finite wavelength about which bifurcation analyses may be developed. Continuing work has shown that a theory of this kind can be developed.

8. Comparison with experiment

Chen *et al.* (1992) remarked that two conditions are satisfied for all known experimental observations of cellular or striped diffusion flames, namely the Lewis number of the more completely consumed reactant is less than a critical value (≈ 0.8), and the diffusion flame is close to extinction as a consequence of either a short residence time, i.e. low Δ, or heat losses to a burner rim. For flames on a Wolfhard–Parker burner, they showed that this result was independent of whether the flame height was controlled by the jet momentum or by buoyancy and of whether the flame was over-ventilated or under-ventilated. Thus, cellular or striped flames should occur when L and Δ are sufficiently low. The latter requirement corresponds to Δ' being sufficiently large, but, of course, less than the value at extinction.

There is qualitatively good agreement of these predictions with the experimental results for several reasons. Within the framework of the current analysis, the existence of cellular or striped flames requires the dispersion relation expressed by the composite expansion given in (35) to exhibit a maximum $\mathrm{Re}(\sigma) > 0$ for some finite k. As shown in figure 7, this condition corresponds to a sufficiently large Δ' and therefore to conditions sufficiently close to extinction. Also, as L approaches unity from $L < 1$, the maximum value of Δ' approaches zero, and thus, according to (36), for σ to remain non-negative k must approach zero, that is, the cell size becomes infinite. As a result, for an experimental apparatus of finite dimension, the cellular instability would be expected to disappear at some value of L less than unity. In the model employed here, the Lewis numbers, and thus the diffusion coefficients, of the two reactants are equal. This indicates that preferential diffusion of a lighter reactant with respect to a heavier reactant is not required to generate the instability, contrary to the proposal of Ishizuka & Tsuji (1981). Moreover, the instability is predicted for any value of A_F, indicating that stoichiometry effects are not critical, contrary to the suggestions of some authors (Dongworth & Melvin 1974). Finally, the instability can occur for any non-zero value of u, provided that Δ is small enough, which is consistent with the finding of Chen *et al.* (1992) that cellular behaviour arises at all flow conditions if the mixture is sufficiently diluted toward extinction and $L < 1$.

From these observations, it is concluded that the predicted conditions for instability are *qualitatively* consistent with the experimental observations. The primary *quantitative* prediction of the theory to be compared with experiments is the transverse wavelength of the cells (ℓ_T), given by (39). Of course, any comparison must be considered approximate because of the differences in boundary conditions between the model and experiments and because the model assumes constant density and transport properties, assumptions that are not satisfied by the experiments. However, an order-of-magnitude comparison of predicted and observed cell sizes will be instructive.

There are several assumptions and estimations that must be made in order to obtain a prediction of ℓ_T. One difficulty is the temperature-dependent nature of many of the parameters, factors that are not considered in our analysis. Here the density (ρ) and flow velocity (U) will be evaluated at the cold-gas conditions, denoted by subscript o, which is considered reasonable because, for the one-dimensional geometry assumed in this paper, if density variations were considered then $\rho U = \rho_o U_o$ would be constant. Since the analysis assumes that the Lewis number L is the same for both

Reference	Measured ℓ_T	Estimated ℓ_T by (39)
Garside & Jackson (1953)	0.7 cm	0.71 cm
Dongworth & Melvin (1974)	1.0 cm	0.37 cm
Ishizuka & Tsuji (1981)	0.7 cm	0.78 cm
Chen *et al.* (1992):		
1. Momentum-dominated blowoff limit		
$U_o = 15$ cm s^{-1} (their figure 5*a*)	0.7 cm	0.71 cm
2. Buoyancy-dominated blowoff limit		
$U_o = 7.1$ cm s^{-1} (their figure 5*b*)	1.6 cm	0.62 cm
3. Heat loss limit		
$U_o = 4.3$ cm s^{-1} (their figure 5*c*)	1.4 cm	0.54 cm

TABLE 1. Measured and predicted values of diffusion flame cell wavelength.

reactants, for these calculations L is taken to be the average of the Lewis numbers of the fuel and oxidant, averaged over the temperature range between ambient and the calculated flame temperature. Another uncertainty lies in assigning a value to ℓ, the domain size, in the light of the fact that all of the experimental configurations employed are essentially semi-infinite in character. A value of ℓ is needed to define the non-dimensional convection velocity u through which the normalizing factor f is determined. Therefore, ℓ will be assigned a value of twice the tube radius for jet flames (Garside & Jackson 1953), a value equal to the slot width for flames stabilized on a Wolfhard–Parker burner (Chen *et al.* 1992), a value of twice the standoff distance for experiments employing a porous cylinder in crossflow (Ishizuka & Tsuji 1981) and a value equal to the transverse width of the channel for flames obtained using the splitter-plate configuration (Dongworth & Melvin 1976). Another difficulty that arises for the jet and Wolfhard–Parker flames is that the flow direction is not orthogonal to the flame front; hence, the component of velocity normal to the front ($U_\perp$) is estimated as $U_o/[1 + 4(h/w)^2]^{1/2}$, where h is the experimental flame height and w the slot or tube width. For the splitter-plate configuration, $U_\perp$ is estimated from the reported flow velocity and the flame angle relative to the splitter plate reported in earlier work using the same burner (Melvin, Moss & Clarke 1971). For the cylinder in crossflow, by design there is a substantial velocity gradient, but reported flame position relative to the stagnation plane and the velocity gradient at the front can be used to estimate $U_\perp$. Given all of these assumptions, in (39) the term $\rho D_T/m$ can be evaluated from $\rho D_T/m \approx \bar{\lambda}/(\bar{c}_p \rho_o U_\perp)$, where the overbars denote temperature-averaged values of the thermal conductivity λ and the specific heat c_p.

To estimate ℓ_T, first the non-dimensional convection velocity $u = m\ell/(2\rho D_T) \equiv \bar{c}_p \rho_o U_\perp \ell/(2\bar{\lambda})$ is determined from the experimental parameters and the estimations of $U_\perp$ and ℓ described above. Then (8) is solved for x_f, the factor f/u is found from (15), and γ is determined from (18) with $T_F = T_O$ set to the ambient temperature. From figure 10, the value of F corresponding to this value of γ is determined; usually γ is negative, but the results are symmetric, that is, $F(-\gamma) = F(\gamma)$. For the purpose of temperature-averaging and to determine the value of $\beta \equiv T_a/T_f^2$, the dimensionless flame temperature T_f is calculated from (9). In the estimation of T_a, an activation energy of $E = 40$ kcal mol^{-1} is chosen for all hydrocarbon-oxygen-diluent mixtures, and $E = 30$ kcal mol^{-1} is chosen for all hydrogen–oxygen–diluent mixtures. A double-iteration procedure is required to solve this set of equations because, in (8) for x_f, u is affected by the flame temperature as a consequence of c_p and λ, which

appear in the definition of u, being functions of temperature, and x_f in turn affects the flame temperature through (9). However, most cases are close enough to limit of large or small u that iterations converge rapidly. With x_f, γ, T_f and β determined by this method, all factors needed to estimate the cell size through (39) are available.

Results of these estimated cell or stripe sizes are given in table 1. It can be seen that, even in the worst case, the difference between the measured and estimated cell size is less than a factor of 3, and in most cases the agreement is much better. Insofar as only order-of-magnitude agreement could be expected considering the differences between the model assumptions and experimental conditions, this level of conformity is considered acceptable and provides further confirmation of the general validity of the model proposed here.

9. Concluding remarks

In this work, a type of linear stability in diffusion flames was analysed by employing a one-dimensional convective diffusion flame as a model. Of particular interest was investigation of the diffusional–thermal instability mechanism by which stripe patterns, observed in near-extinction diffusion flames, can be formed in a convective environment through a coupling of finite-rate chemical reaction with differential diffusion of thermal and chemical energies for Lewis numbers less than unity. With attention focused on the diffusion-flame regime of activation-energy asymptotics (Liñán 1974), the results showed that the instability can begin at finite values of the wavenumber if the flame is sufficiently close to quasi-steady extinction. Reasonable agreement was obtained with stripe patterns observed in the experiments.

An immediate extension of the present analysis can be made to diffusion-flame instabilities with the Lewis numbers greater than unity. Of particular interest would be to explain oscillatory evolution of the flame temperature, demonstrated in the early numerical study by Kirkby & Schmitz (1966), which eventually led to extinction. This entails the complication of computing complex dispersion relations, as opposed to the real ones obtained here. Comparison of the characteristics of these oscillatory instabilities with those known for premixed flames could help in further identifying fundamental differences between premixed and non-premixed combustion.

There is also interest in instability mechanisms of diffusion flames that lead to periodic wrinkling of the reaction sheet rather than to the periodic local quenching addressed here. The premixed-flame regime of activation-energy asymptotics (Liñán 1974) can exhibit this type of instability for near-extinction diffusion flames having small values of the stoichiometric mixture fraction, a situation which is often encountered in practical combustion systems. Since leakage of the deficient reactant then occurs at the leading order, the reaction-sheet location can depart from its unperturbed steady-state location by a distance of the order of the characteristic convective–diffusive thickness. A method analogous to that employed to describe cellular instability of premixed flames (Sivashinsky 1977; Joulin & Clavin 1979) can be applied to analyse this type of diffusion-flame instability. Although the presence of heat loss and near-extinction conditions suggests that the characteristics of the instability will resemble those found in non-adiabatic premixed flames (Joulin & Clavin 1979), a systematic analysis is needed to distinguish possible cellular-instability characteristics that are peculiar to diffusion flames in this regime.

Finally, it would now be worth pursuing nonlinear bifurcation analyses for the present problem, as well as for that of the premixed-flame regime. If wrinkling of the reaction sheet occurs in diffusion flames, then the resulting increase in the

reaction surface area may lead to a decrease in the average scalar dissipation rate and thereby result in flames more resistant to extinction. As has already been shown in nonlinear stability analyses of non-adiabatic premixed flames (Joulin & Sivashinsky 1983; Joulin 1986), wrinkling can achieve extended flammability limits. Similarly, with the locally quenched diffusion flames approached in the present paper, although the weak segments of the reaction sheet are quenched even before quasi-steady extinction, the strong segments may sustain strain rates appreciably greater than the extinction strain rate because of their enhanced reaction rate. Because of the need to find suitable local scalings in the vicinity of the bifurcation point, development of the bifurcation analysis corresponding to the present problem could pose interesting challenges. Such analyses will be easier with convective–diffusive scaling when Lewis numbers differ from unity by amounts of the order of the reciprocal of the Zel'dovich number.

The authors would like to thank Professors Amable Liñán, Paul Clavin and Pedro Garcia-Ybarra for many helpful discussions and Professor Satoru Ishizuka for providing us with unpublished experimental results. The contribution of the authors to this research was supported as follows: J.S.K. and F.A.W. by the National Science Foundation Grant No. CTS 95-26410, and P.D.R. by NSF Presidential Young Investigator Award Grant No. CBT-8657223 and NASA-Lewis Grant No. NAG3-1523.

Appendix A. Method for calculating the derivative of the inner-layer structure with respect to reactant leakage

Accurate results for Δ' are needed in (24) for using the dispersion relation. In principle, Δ' may be obtained by solving the problem defined in (19) for various values of Δ and then differentiating numerically. However, this is quite inaccurate, and therefore the alternative procedure described here is employed. This procedure turns out to be needed for finding other quantities associated with dispersion relations as well, as will be seen in the following Appendices.

To determine the influence of the fluctuation of the fuel leakage α_F, we must calculate various derivatives of the inner-layer flame structure with respect to α_F. This involves expansion of (19) to include a perturbation of α_F about a given value α_F^0. Since θ and Δ are parametrically dependent on α_F, letting α_F' denote a small increment in α_F, we may write

$$\left.\begin{aligned} &\alpha_F = \alpha_F^0 + \alpha_F', \\ &\theta(\xi;\alpha_F) = \Theta(\xi;\alpha_F^0) + \frac{\partial\theta}{\partial\alpha_F}(\xi;\alpha_F^0)\,\alpha_F' + \cdots = \Theta(\xi;\alpha_F^0) + \vartheta\,\alpha_F' + \cdots, \\ &\Delta(\alpha_F) = \Delta(\alpha_F^0) + \left.\frac{\mathrm{d}\Delta}{\mathrm{d}\alpha_F}\right|_{\alpha_F=\alpha_F^0} \alpha_F' + \cdots = \Delta_0\,(1 + \Delta'\,\alpha_F' + \cdots), \end{aligned}\right\} \tag{A 1}$$

where

$$\vartheta \equiv \left.\frac{\partial\theta}{\partial\alpha_F}\right|_{\alpha_F=\alpha_F^0}, \quad \Delta' \equiv \left.\frac{\mathrm{d}\ln\Delta}{\mathrm{d}\alpha_F}\right|_{\alpha_F=\alpha_F^0}, \quad \Delta_0 \equiv \Delta(\alpha_F^0). \tag{A 2}$$

Substituting the above expansions into (19) and collecting the terms at order α_F' alone,

we find the problem for determining ϑ for $m = n = 1$ to be

$$\left.\begin{aligned} \frac{\mathrm{d}^2\vartheta}{\mathrm{d}\xi^2} &= \Lambda_0\,\mathrm{e}^{-(\Theta+\gamma\xi)}\left[(2\Theta-\Theta^2+\xi^2)\,\vartheta+\Lambda'(\Theta^2-\xi^2)\right], \\ \frac{\mathrm{d}\vartheta}{\mathrm{d}\xi} &\to 0 \quad \text{as} \quad \xi\to\pm\infty. \end{aligned}\right\} \tag{A 3}$$

To (A 3) must be appended a supplementary condition to assure that the matching condition for the fuel leakage, $\alpha_F = (\theta-\xi)|_{\xi\to\infty}$, is satisfied:

$$\alpha_F^0+\alpha_F' = \Theta(\xi;\alpha_F^0)+\vartheta\,\alpha_F'-\xi \quad \text{as} \quad \xi\to\infty. \tag{A 4}$$

Since $\alpha_F^0 = (\Theta-\xi)|_{\xi\to\infty}$, the applicable supplementary condition for (A 3) is then found to be

$$\vartheta \to 1 \quad \text{as} \quad \xi\to\infty. \tag{A 5}$$

Solution to (A 3) with the additional condition in (A 5) yields a unique function ϑ, the eigenvalue Λ' and a constant value for $\vartheta(-\infty)$ which corresponds to $r = \mathrm{d}\alpha_O/\mathrm{d}\alpha_F$, required in the dispersion relation. For $\gamma = 0$, $r = 1$ for all values of α_F, and corresponding numerical results for Λ' are shown in figure 3, along with results for two other values of γ.

Appendix B. Onset condition of fast-time instability for planar disturbances

The eigenvalue problem describing fast-time instability for $K = 0$ with general Lewis number can be written from (31) as

$$\left.\begin{aligned} &\frac{\mathrm{d}^2\psi}{\mathrm{d}\xi^2}-S\,\psi = \frac{\mathrm{d}^2\chi}{\mathrm{d}\xi^2}-LS\,\chi = \Lambda\,\mathrm{e}^{-(\Theta+\gamma\xi)}\left[2\Theta\chi-(\Theta^2-\xi^2)\psi\right], \\ &\frac{\mathrm{d}\psi}{\mathrm{d}\xi} \to \mp S^{1/2}\psi, \quad \frac{\mathrm{d}\chi}{\mathrm{d}\xi} \to \mp(LS)^{1/2}\chi \quad \text{as} \quad \xi\to\pm\infty. \end{aligned}\right\} \tag{B 1}$$

Here we are seeking the condition at which the largest eigenvalue S begins to be positive.

Considering a situation immediately after the onset of fast-time instability, we assume that S is a small positive number. If $S^{1/2}$ is employed as a small expansion parameter, the eigenvalue problem becomes, at the leading order,

$$\frac{\mathrm{d}^2\psi}{\mathrm{d}\xi^2} = \frac{\mathrm{d}^2\chi}{\mathrm{d}\xi^2} = \Lambda\,\mathrm{e}^{-(\Theta+\gamma\xi)}\left[2\Theta\chi-(\Theta^2-\xi^2)\psi\right], \tag{B 2}$$

which now has a coupling function for $\psi-\chi$ in a linear functional form. The slope and integration constant for the coupling function are obtained by imposing the matching condition. In order to achieve matching, it must be noted that decay of the solution to zero takes place in an outer region with thickness of order $1/S^{1/2}$ in the ξ-coordinate. In terms of the coordinate $\zeta = S^{1/2}\xi$, the differential equations in the outer layer become

$$\frac{\mathrm{d}^2\psi}{\mathrm{d}\zeta^2}-\psi = 0, \quad \frac{\mathrm{d}^2\chi}{\mathrm{d}\zeta^2}-L\,\chi = 0. \tag{B 3}$$

The exponentially decaying outer solutions are found to be

$$\psi = \begin{cases} \psi^+\,\mathrm{e}^{-\zeta} \\ \psi^-\,\mathrm{e}^{\zeta}, \end{cases} \qquad \chi = \begin{cases} \chi^+\,\mathrm{e}^{-L^{1/2}\zeta} \\ \chi^-\,\mathrm{e}^{L^{1/2}\zeta}, \end{cases} \qquad \text{for} \quad \begin{cases} \zeta>0 \\ \zeta<0, \end{cases} \tag{B 4}$$

where the integral constants $\psi^{\pm}$ and $\chi^{\pm}$ are yet to be determined.

In the double limit of $\zeta \to \pm 0$ and $\xi \to \pm\infty$, matching is achieved to yield $\psi^+ - \psi^- = \chi^+ - \chi^-$ and $\psi^+ + \psi^- = L^{1/2}(\chi^+ + \chi^-)$, and a unique coupling function at leading order is found to be

$$\psi - \chi = (L^{1/2} - 1)\frac{\chi^+ + \chi^-}{2}. \tag{B 5}$$

The value of χ^+ can be chosen arbitrarily because the problem is linear and homogeneous. With the choice of $\chi^+ = 1$, the resulting eigenvalue problem, written in terms of χ, becomes

$$\left.\begin{aligned} \frac{\mathrm{d}^2\chi}{\mathrm{d}\xi^2} = \Delta\, \mathrm{e}^{-(\Theta+\gamma\xi)}\left[(2\Theta - \Theta^2 + \xi^2)\chi + \frac{1+\chi^-}{2}(1 - L^{1/2})(\Theta^2 - \xi^2)\right], \\ \chi \to 1 \quad \text{as} \quad \xi \to \infty, \quad \chi \to \chi^- \quad \text{as} \quad \xi \to -\infty. \end{aligned}\right\} \tag{B 6}$$

Comparison of this equation with (A 3) and (A 5) shows that $\chi^- = r$ and that an eigensolution exists if $\Delta' = (1 - L^{1/2})(1 + r)/2$. Although the eigenfunction χ must approach zero as $\xi \to \pm\infty$, that of (B 6) approaches non-zero constant values, $\chi|_{\xi\to\infty} \to 1$ and $\chi|_{\xi\to-\infty} \to r$. The composite expansion of the inner and exponentially decaying outer solutions, however, provides an eigenfunction that is uniformly valid throughout the entire range of ξ and that exhibits the correct exponential decay at infinity. Since this eigensolution exists only near the onset of instability, the onset condition of fast-time instability for the planar wave is

$$\Delta' = (1 - L^{1/2})\frac{1+r}{2}. \tag{B 7}$$

Appendix C. Asymptotic behaviour of fast-time instability for large wavelengths

The asymptotic behaviour of the maximum value of S for small K is obtained here. Since S is linear in K^2 as $K \to 0$, the asymptotic relation is sought in the form

$$S = CK^2. \tag{C 1}$$

Upon substituting this relation into (31), a set of differential equations is obtained, which along with the relevant boundary conditions leads to the problem

$$\left.\begin{aligned} \frac{\mathrm{d}^2\psi}{\mathrm{d}\xi^2} - (1+C)K^2\psi = \frac{\mathrm{d}^2\chi}{\mathrm{d}\xi^2} - (1+LC)K^2\chi = \Delta \mathrm{e}^{-(\Theta+\gamma\xi)}\left[2\Theta\chi - (\Theta^2 - \xi^2)\psi\right], \\ \frac{\mathrm{d}\psi}{d\xi} \to \mp\left[(1+C)K^2\right]^{1/2}\psi, \quad \frac{\mathrm{d}\chi}{\mathrm{d}\xi} \to \mp\left[(1+LC)K^2\right]^{1/2}\chi \quad \text{as} \quad \xi \to \pm\infty. \end{aligned}\right\} \tag{C 2}$$

Here we can follow the same perturbation method that was used in the previous Appendix. If $\left[(1+C)K^2\right]^{1/2}$ is employed as a small expansion parameter, then an asymptotic solution is found to exist when

$$\Delta' = \frac{1+r}{2}\left[1 - \left(\frac{1+LC}{1+C}\right)^{1/2}\right]. \tag{C 3}$$

The asymptotic relation given in (34) is obtained from (C 1) by solving (C 3) for C.

As an improvement to (34), a two-term expansion of the dispersion relation can be

found near the turning point of Λ by utilizing the fact that the critical value of K, denoted by K_c, at which S returns to zero from being positive is independent of L as shown in figure 9. If the values $S = 0$ and $K = K_c \neq 0$ are substituted into (31), then the equation reduces to

$$\frac{\mathrm{d}^2\psi}{\mathrm{d}\xi^2} - K_c^2\psi = V(\xi)\psi, \quad \frac{\mathrm{d}\psi}{\mathrm{d}\xi} \to \mp(K_c^2)^{1/2}\psi \quad \text{as} \quad \xi \to \pm\infty, \tag{C 4}$$

where the potential $V(\xi)$ is

$$V(\xi) = \Lambda\,\mathrm{e}^{-(\Theta+\gamma\xi)}(2\Theta - \Theta^2 + \xi^2), \tag{C 5}$$

and use has been made of the coupling function $\psi - \chi = 0$. Since we are looking for solutions near the turning point, the perturbation of the fuel leakage from that at the condition of minimum Λ is considered to be a small expansion parameter $\delta = \alpha_F - \alpha_{F,m}^0$, where the subscript m denotes conditions at the minimum Λ. In the vicinity of the minimum, the variables are expanded as

$$\left.\begin{aligned} \Lambda &= \Lambda_m\left[1 + \delta^2\,\tfrac{1}{2}\Lambda_m'' + \cdots\right], \\ K_c^2 &= \delta\kappa^2 + \cdots, \\ \psi &= \psi_0 + \delta\psi_1 \cdots, \\ \Theta &= \Theta_m + \delta\vartheta_m + \cdots, \end{aligned}\right\} \tag{C 6}$$

where $\vartheta_m = (\partial\Theta/\partial\alpha_F)|_{\Lambda'=0}$ and $\Lambda_m'' = \Lambda_m^{-1}(\mathrm{d}^2\Lambda/\mathrm{d}\alpha_F^2)|_{\Lambda'=0}$. When these expansions are substituted into (C 4), the problems at the first two orders in δ become

$$\frac{\mathrm{d}^2\psi_0}{\mathrm{d}\xi^2} - V_0(\xi)\psi_0 = 0, \quad \psi_0 \to 0 \quad \text{as} \quad \xi \to \pm\infty, \tag{C 7}$$

and

$$\frac{\mathrm{d}^2\psi_1}{\mathrm{d}\xi^2} - V_0(\xi)\psi_1 = [\kappa^2 + V_1(\xi)]\psi_0, \quad \psi_1 \to 0 \quad \text{as} \quad \xi \to \pm\infty, \tag{C 8}$$

where the potentials at each order are

$$\left.\begin{aligned} V_0(\xi) &= \Lambda_m\,\mathrm{e}^{-(\Theta_m+\gamma\xi)}(2\Theta_m - \Theta_m^2 + \xi^2), \\ V_1(\xi) &= \Lambda_m\,\mathrm{e}^{-(\Theta_m+\gamma\xi)}(2 - 4\Theta_m + \Theta_m^2 - \xi^2)\,\vartheta_m. \end{aligned}\right\} \tag{C 9}$$

Equation (C 7) yields the eigenfunction at the bifurcation point. As summarized in the previous Appendix, the eigenfunction ψ_0 is then given by ϑ_m in the inner layer and by the first expression in (B 4) in the outer layer if $\zeta \equiv K_c\xi$. A uniformly valid eigenfunction may then be constructed from a composite expansion, as before. On the other hand, (C 8) is an inhomogeneous linear (self-adjoint) differential equation, and a solution exists if the projection of the inhomogeneous part to the null space of the corresponding homogeneous differential equation vanishes. Since the null solution of the homogeneous differential equation is ψ_0, the solvability condition can be written as

$$\kappa^2\int_{-\infty}^{\infty}\psi_0^2\,\mathrm{d}\xi + \int_{-\infty}^{\infty}V_1(\xi)\psi_0^2\,\mathrm{d}\xi = 0. \tag{C 10}$$

When the integrals are evaluated, care must be taken, since the exponential decay of the eigenfunction ψ_0 occurs in the outer layer, whose rescaled coordinate is given by $\zeta = \delta^{1/2}\kappa\xi$. The first-order potential $V_1(\xi)$ has a weighting function $\mathrm{e}^{-(\Theta+\gamma\xi)}$, giving exponential decay of the integrand for large ξ, so that rescaling of the coordinate is

not necessary to find the second integral in (C 10). On the other hand, most of the contribution to the first integral comes from the decaying tail in the outer region. This integral is then found to be

$$\int_{-\infty}^{\infty} \psi_0^2 \, \mathrm{d}\xi = \frac{1 + r_m^2}{2\delta^{1/2}\kappa}, \tag{C 11}$$

where r_m is the value of r at the minimum Δ.

These results enable the two-term expansion of the dispersion relation to be evaluated explicitly. When the relationship $\Delta' = (\alpha_F - \alpha_{F,m}^0)\Delta_m''$ is used to evaluate the small parameter δ, the asymptotic expression for K_c in terms of Δ' is found from (C 6), (C 10) and (C 11) to be given by

$$K_c^2 = \left[\frac{2\Lambda}{\Delta_m''(1 + r_m^2)}\right]^2 \Delta'^2, \tag{C 12}$$

where a positive constant of order unity has been defined as

$$\Lambda = -\int_{-\infty}^{\infty} V_1(\xi)\,\psi_0^2 \, \mathrm{d}\xi = \int_{-\infty}^{\infty} \Delta_m \, \mathrm{e}^{-(\Theta_m + \gamma\xi)} (\xi^2 - \Theta_m^2 + 4\Theta_m - 2)\, \vartheta_m^3 \, \mathrm{d}\xi. \tag{C 13}$$

For $\gamma = 0$, $\Delta_m'' = 0.823$, and numerical integration shows that $\Lambda = 1.87$. Figure 10 shows Λ and Δ_m'' as functions of γ, obtained from numerical integrations. In terms of the value of K_c thus determined from (C 12), the two-term expansion of the dispersion relation near the minimum of Δ is found by using (34) to be

$$S = \frac{4\Delta' K^2}{(1 + r)(1 - L)} \left(1 - \frac{K^2}{K_c^2}\right). \tag{C 14}$$

REFERENCES

BARENBLATT, G. I., ZEL'DOVICH, Y. B. & ISTRATOV, A. G. 1962 On diffusional-thermal stability of a laminar flame. *Prikl. Mekh. Tekhn. Fiz.* **4**, 21–26 (in Russian).

BUCKMASTER, J. D. 1992 Flame instability. In *Major Research Topics in Combustion* (ed. M. Y. Hussaini, A. Kumar & R. G. Voigt). Springer.

BUCKMASTER, J. D. & LUDFORD, G. S. S. 1982 *Theory of Laminar Flames*. Cambridge University Press.

BUCKMASTER, J. D., NACHMAN, A. & TALIAFERRO, S. 1983 The fast time instability of diffusion flames. *Physica* **9D**, 408–424.

CHEN, R., MITCHELL, G. B. & RONNEY, P. D. 1992 Diffusive-thermal instability and flame extinction in nonpremixed combustion. In *Twenty-Fourth Symp. (Intl) on Combustion*, pp. 213–221. The Combustion Institute, Pittsburgh, PA.

CHUNG, S. H. & LAW, C. K. 1983 Structure and extinction of convective diffusion flames with general Lewis numbers. *Combust. Flame* **52**, 59–79.

CLAVIN, P. 1985 Dynamic behavior of premixed flame fronts in laminar and turbulent flows. *Prog. Energy Combust. Sci.* **11**, 1–59.

DARRIEUS, G. 1938 Propagation d'un front de flamme. Unpublished works presented at La Technique Moderne (and at Congrés de Mécanique Appliquée Paris, 1945).

DONGWORTH M. R. & MELVIN, A. 1976 The transition to instability in a steady hydrogen-oxygen diffusion flame. *Combust. Sci. Technol.* **14**, 177–182.

GARSIDE, J. E. & JACKSON, B. 1953 The formation and some properties of polyhedral burner flames. In *Fourth Symp. (Intl) on Combustion*, pp. 545–552. The Williams and Wilkins Co. Baltimore, MD.

ISHIZUKA, S. & TSUJI, H. 1981 An experimental study of effect of inert gases on extinction of laminar diffusion flames. In *Eighteenth Symp. (Intl) on Combustion*, pp. 213–221. The Combustion Institute, Pittsburgh, PA.

JOULIN, G. 1986 Shapes, velocities and propagation limits of a non-adiabatic cellular flame. *Combust. Sci. Technol.* **47**, 69–79.

JOULIN, G. & CLAVIN, P. 1979 Linear stability analysis of nonadiabatic flames: diffusional-thermal model. *Combust. Flame* **35**, 139–153.

JOULIN, G. & SIVASHINSKY, G. I. 1983 On the dynamics of nearly-extinguished non-adiabatic cellular flames. *Combust. Sci. Technol.* **31**, 75–90.

KIRKBY, L. L. & SCHMITZ, R. A. 1966 An analytical study of the stability of a laminar diffusion flame. *Combust. Flame* **10**, 205–220.

LANDAU, L. 1944 On the theory of slow combustion. *Acta Physicochimica URSS* **19**, 77–85.

LAW, C. K. & CHUNG, S. H. 1982 Steady state diffusion flame structure with Lewis number variations. *Combust. Sci. Technol.* **29**, 129–145.

LIÑÁN, A. 1974 The asymptotic structure of counterflow diffusion flame for large activation energies. *Acta Astronautica* **1**, 1007–1039.

MELVIN, A., MOSS, J. B. & CLARKE, J. F. 1971 The structure of a reaction-broadened diffusion flame. *Combust. Sci. Technol.* **4**, 17–30.

MORSE, P. M. & FESHBACH, H. 1953 *Methods of Theoretical Physics.* pp. 766–769. McGraw-Hill.

PETERS, N. 1978 On the stability of Liñán's "premixed flame regime". *Combust. Flame* **33**, 315–318.

SESHADRI, K. & TREVIÑO, C. 1989 The influence of the Lewis numbers of the reactants on the asymptotic structure of counterflow and stagnant diffusion flames. *Combust. Sci. Technol.* **64**, 243–261.

SIVASHINSKY, G. I. 1977 Diffusional-thermal theory of cellular flames. *Combust. Sci. Technol.* **15**, 137–146.

STEWART, D. S. 1986 On the stability of the reaction zone of the plane deflagration. *Combust. Flame* **64**, 157–165.

STEWART, D. S. & BUCKMASTER, J. D. 1986 The stability of Liñán's "premixed flame regime" revisted. *SIAM J. Appl. Maths* **46**, 582–587.

TAYLOR, G. I. 1950 The instability of liquid surfaces when accelerated in a direction perpendicular to their planes. I. *Proc. R. Soc. Lond.* A **201**, 192–196.

TITCHMARSH, E. C. 1946 *Eigenfunction Expansions Associated with Second-Order Differential Equations*, pp. 107-128. Clarendon Press.

TURING, A. M. 1952 The chemical basis of morphogenesis. *Phil. Trans. R. Soc. Lond.* B **237**, 37–72.